



UNITED NATIONS  
UNIVERSITY

**UNU-GTP**

Geothermal Training Programme

Orkustofnun, Grensasvegur 9,  
IS-108 Reykjavik, Iceland

Reports 2019  
Number 8

## **BOREHOLE GEOLOGY OF WELL FIALE 3, ASAL-FIALE GEOTHERMAL FIELD, DJIBOUTI**

**Araksan Ahmed Aden**

Office Djiboutien de Développement de l'Energie Géothermique (ODDEG)

Presidency of the Republic, Road PK20

P.O. Box: 2025, Djibouti

REPUBLIC OF DJIBOUTI

*araksan\_ahmed@yahoo.fr ; aden@unugtp.is*

### **ABSTRACT**

The geothermal well Fiale-3 is in the Asal-Fiale geothermal field in the north-western part of the Fiale caldera. The well is directionally drilled to a total measured depth of 2660 m in a N224° direction. To provide information about the stratigraphy, thermal conditions, and a detailed description of the geothermal reservoir characteristics of the well, binocular microscopy, thin section petrography, XRD analyses and methylene blue analyses have been carried out. The lithostratigraphy of Fiale-3 is formed by four main stratigraphic units, which are the Asal series, the Afar stratoid series, the Dalha basalt series and the Mabla rhyolite. Several alteration minerals have been observed with progressive depth and the occurrence of hydrothermal alteration minerals is related to their formation temperatures such as smectite ( $\geq 40^{\circ}\text{C}$ ), quartz ( $\geq 180^{\circ}\text{C}$ ), chlorite ( $\geq 220^{\circ}\text{C}$ ), epidote ( $\geq 230^{\circ}\text{C}$ ), and actinolite ( $\geq 280^{\circ}\text{C}$ ). Further, anhydrite has also been observed from 700 m onwards. Anhydrite as a sulphate mineral is a good indicator for seawater infiltration. In total, five alteration zones can be classified. These are an unaltered zone (0-145 m), a smectite zone (145-550 m), a chlorite zone (550-792 m), an epidote zone (792-1283 m), and an epidote-actinolite zone (1283-2660 m). However, the observed alteration pattern does not present the thermal conditions today. Measured temperatures in the well from downhole logging indicate a temperature reversal between 733 and 1700 m measured depth (MD) due to a large inflow of cold seawater through the NW-SE major faults of the rift. The absence of low-temperature minerals in the reversal zone may indicate that the geothermal system has not been equilibrated. This may indicate that the cooling is relatively recent. Permeable zones are identified from circulation losses and temperature logs. The largest feed zone at 733 m (MD) is mainly controlled by the rift faults which led to the inflow of cold seawater into the system. In general, the well shows a relative low permeability in the shallow and deep reservoir. The alteration and temperature models of the Asal-Fiale geothermal field provide no evidence for the existence of an upflow.

### **1. INTRODUCTION**

The Republic of Djibouti is a territory of 23 000 km<sup>2</sup> located in East Africa. The country is situated in the south-eastern part of the Afar depression where three large-scale rift/ridge zones form an active triple-junction (Courtilot et al., 1987). The three zones are the intracontinental East African Rift, the

oceanic ridges of the Red Sea and the Gulf of Aden. The major rifting creates several disconnected rift segments that are stretching the crust and the lithosphere within the Afar rift (Tapponnier et al., 1990). The Asal-Ghoubbet rift is one of the emergent segments of the Aden Gulf ridge which spreads westward on land into the Afar depression (Manighetti et al., 1998). Different volcanic features associated with effusive events separated in time characterize the rift-in-rift area. One of them is the former central volcano Fiale that is characterized by a caldera structure. The Fiale caldera is the studied area in this report (Figure 1). Still today, the area is subject to seismic activity and the fumaroles and hot springs are active.

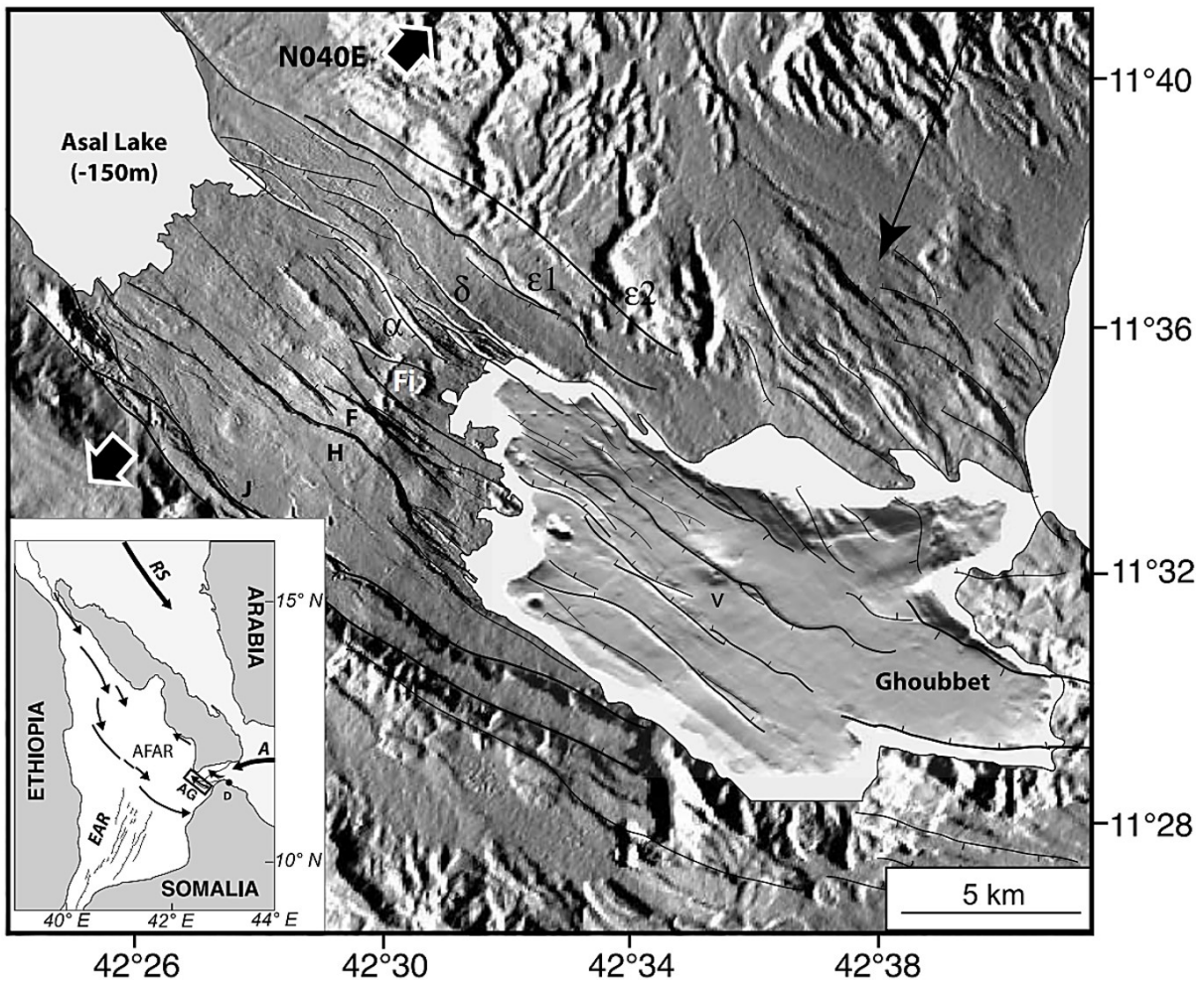


FIGURE 1: Topographic and tectonic map of Asal-Ghoubbet rift. Faults ( $\alpha$ ,  $\delta$ ,  $\epsilon_1$  and  $\epsilon_2$ , F, H, J, K) taken from Manighetti et al. (2001a, 2001b) and Audin et al. (2001). Fi stands for the Fiale caldera; v for the easternmost recent volcano in Ghoubbet and AG-T for Asal-Ghoubbet/Tadjoura transfer faults. The inset shows the general setting of the Afar depression, at junction between the East African Rift (EAR), the Red Sea Ridge (RS), and the Aden Ridge (A). D stands for Djibouti and arrows symbolize propagating, active rift segments. The Asal-Ghoubbet rift (AG) is indicated by a rectangle

Geothermal exploration in Djibouti began in 1970. Geological, geochemical and geophysical studies have been undertaken to locate possible areas for geothermal development and exploration by the French Geological Survey BRGM (1973). In 1975, the first two exploration wells were drilled in the southwestern part of the Asal-Ghoubbet rift. In 1987, four more deep wells had been drilled in the area (Aquater, 1989). Twenty years later in 2008, a complete TEM and MT campaign covering the Asal area was carried out by the Iceland GeoSurvey (ÍSOR) for REI (Reykjavik Energy Invest) which showed the

existence of three separate geothermal fields, which are Gale le Koma, Asal NW in the south of Lake Asal, and Asal-Fiale named after the Fiale caldera edifice (Doubre et al, 2007; Árnason et al, 2008).

The Asal-Fiale area was chosen in 2011 to be the location of three new deviated wells with a large production diameter of 9 5/8" (AfDB, 2013). In the long term, the objective is to build a power plant able to produce 50 MW to support the increasing energy needs of the country. The drilling of the first well, Fiale 1, was launched on the 18<sup>th</sup> of July 2018. Three directional wells have been completed in the area with the following measured depths (MD): 2745 m for Fiale 1, 2705 m for Fiale 2 and 2660 m for Fiale 3.

The objective of this study is to elaborate the subsurface stratigraphy and thermal conditions and to establish a detailed description of the geothermal reservoir of the well Fiale 3. For this purpose, several analyses have been undertaken. They include the analysis of cuttings under binocular microscope, and the analysis of hydrothermal alteration minerals and their paragenesis. The classification and location of the alteration zones and the impact of the large inflow of cold water have been studied with the help of X-ray diffraction (XRD) and petrographic analysis. Finally, the study of the temperature profile and the correlation of the lithostratigraphy and the alteration minerals between Fiale 3 and the surrounding wells will provide a better understanding of the geothermal system in the Fiale caldera.

## 2. GEOLOGICAL SETTING

Located in the eastern part of the African continent, the Afar depression is the result of 30 million years of separation of the continental plates of Arabia and Africa caused by the rise of a mantle plume in the lithosphere (Courtilot et al, 1999). The area is characterized by different active rifts. The Asal-Ghoubbet rift is one of the emergent segments of the Aden Gulf ridge which spreads westward on land into the Afar depression (Manighetti et al., 1998). It is one of the youngest rifts within the Afar region (0.9 Ma) (Varet, 1978) and is ~40 km long and only a 15 km section is emerged in NW-SE direction. It opens at a rate of  $15 \pm 2$  mm/year in  $N40^\circ \pm 5^\circ E$  direction (De Chabaliér and Avouac, 1994). The rift extends from the Gulf of Ghoubbet in the SE to Lake Asal in the NW. Moreover, the emerged part shows a dense network of fissures and sub-vertical normal faults with a strike of  $N130^\circ \pm 10^\circ$  running from the northwest shore of the Lake Asal to the Ghoubbet basin, as shown in Figure 1 (Manighetti et al., 1998).

The rift-in-rift area has witnessed magmatic and tectonic activities over its whole evolution. Different phases of volcanic activity have alternated with phases of major faulting (Stein et al., 1991). The period between  $853 \pm 35$  ka to  $315 \pm 53$  ka allowed the formation of hyaloclastites (submarine pyroclastic rocks). During that time the rift was below sea level ( $326 \pm 15$  ka) in the southern part of the rift and magmatic activity remained effusive in the north ( $334 \pm 43$  ka and  $315 \pm 53$  ka). During this first period, faulting has dismantled the lava formations (Manighetti et al., 1998). Between ~300 and 100 ka, the volcanic activity in the area was concentrated on the central shield volcano Fiale. The inner floor and previous faults have been filled and covered by large basalt lava flows (Pinzuti, 2006). These lava flows might have their origin in a long-lived, deep magma chamber (Ngoc et al., 1981). Then, an "a-magmatic" period of 100 ka long followed. This period is characterized by a high faulting activity that progressively dismantled the lava piles including the Fiale edifice. Only short phases of fissure eruptions occurred at this time, such as those responsible of the recent lava fields on either side of the Fiale volcano (De Chabaliér and Avouac, 1994). The decrease of magmatic activity caused the previous basalt lava flows that structure the Fiale volcano to become gradually offset by normal faults. The development of the modern rift started 40 to 30 ka ago and the northernmost faults ( $\alpha$  to  $\delta$ ) are the youngest and presently the most active (Figure 1) (Manighetti et al., 1998). During this tectonic period, the Fiale volcano collapsed and formed the ~1.5 km wide circular caldera known today. The rare magmatic activities were located within the inner floor together with small volcanic edifices and fissure eruptions (Stein et al., 1991).



The most recent magmatic activity occurred in November 1978 (Abdallah et al., 1979). A major rifting episode associated with two large earthquakes in the Ghoubbet (mb 5 and 5.3) and a one week-long basaltic fissure eruption at the north-western tip of the volcanic chain gave birth to the Ardoukoba volcano (ISERST et al., 1980). According to Ruegg (1979), this episode led to a 2 m extension of the rift along the N40°E direction and a subsidence of 70 cm of the inner floor. Mechanical modelling of the deformation suggests that the rifting episode might be linked to the sudden opening of two 4 to 8 km long dykes at ~ 4–5 km depth in the rift's inner floor, the larger one being located in the Ghoubbet rift (Tarantola et al., 1979, 1980).

In general, the Asal-Ghoubbet rift is the result of a major NW-SE trending extensional regime with numerous faults and fractures. Two major asymmetric faults show a typical graben structure. Several other fault trends have also been identified in the area such as E-W faults resulting from rifting during the Miocene in the Gulf of Aden and later in Tadjoura (Khodayar, 2008), N-S faults, and rare ENE faults. Based on the geological map of the rift (Figure 2), the more recent basaltic formations are hyaloclastite and lacustrine deposits in the inner part while the oldest basalts, Stratoid basalts, are found in the external part.

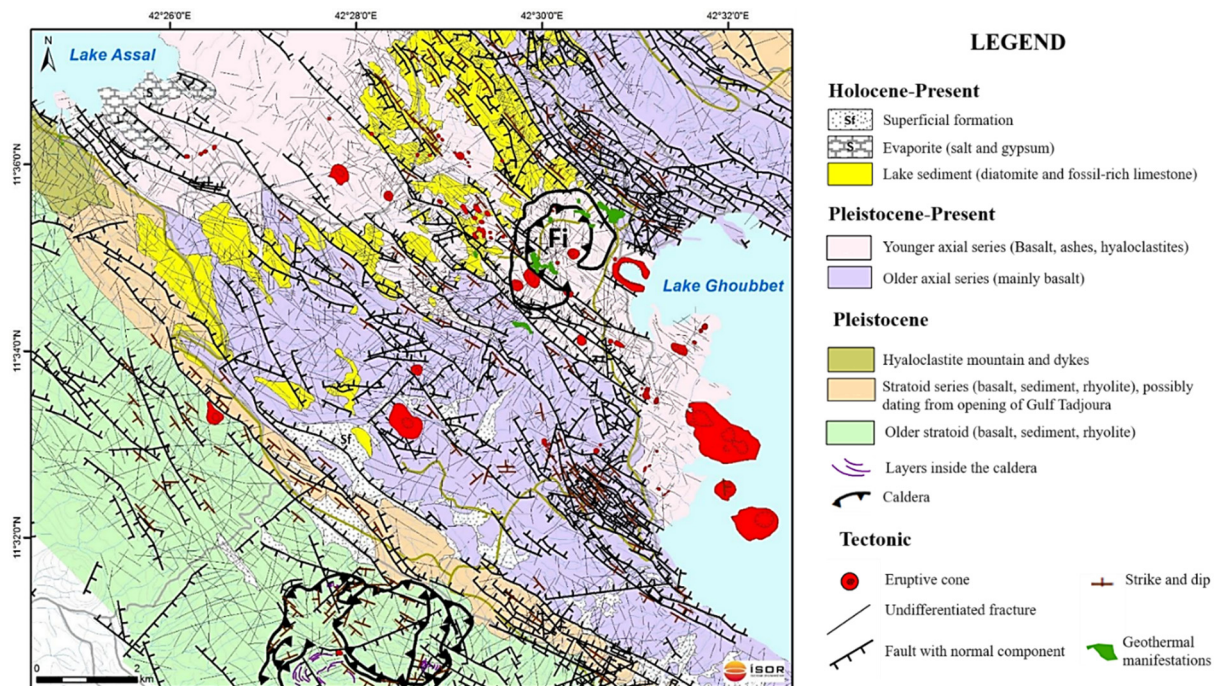


FIGURE 2: Geological map of the Asal-Ghoubbet rift between the gulf of Ghoubbet and Lake Asal, Fi stands for the Fiale caldera (from Khodayar, 2008). The structural settings are characterized by NW-SE trending rift faults and NE-SW trending transform faults

### 3. ASAL-FIALE GEOTHERMAL AREA

#### 3.1 Geological review

The Fiale caldera is in the Asal-Ghoubbet rift axial graben between two boundary rift faults trending NW. It is a former volcano that has been active from ~ 300 to 80 ka (Manighetti et al., 1998). The inner part of the caldera is covered by young basaltic lava flows forming the so-called Lava Lake. The Fiale caldera is surrounded by a 1.5 km diameter rim that measures 20 to 30 m high. It is cut by a dense network of approximately EW to NW striking open fissures and small normal faults. The Fiale caldera is almost entirely enclosed in that graben.



Seismological studies carried out by Doubre et al. (2007) shed light on the transient magma-tectonic mechanisms that contribute to the rifting cycle. According to them, a main volcanic plumbing system is located at the centre of the rift under the Fiale caldera. It corresponds to the focused zone of crustal production where a magma chamber is suspected. The whole caldera zone is found overlaying a 2 km wide central column of low seismic velocities that suggests the presence of hot intrusions above a deeper magma chamber at 5 to 6 km depth. Doubre et al. (2007) showed that the seismicity in the Fiale volcanic system zone occurs in successive crises (Figure 3). These latter are local seismic events observed at the basis of the faults. These events are caused by up and down vertical motions along the faults, especially along the Fiale ring faults in the east. The piston-like motions are likely related to inflation-deflation motions in the underlying magma reservoir and intrusions. Thereby, the probable presence of a magma chamber at shallow depth could represent the heat source of a geothermal system within the area.

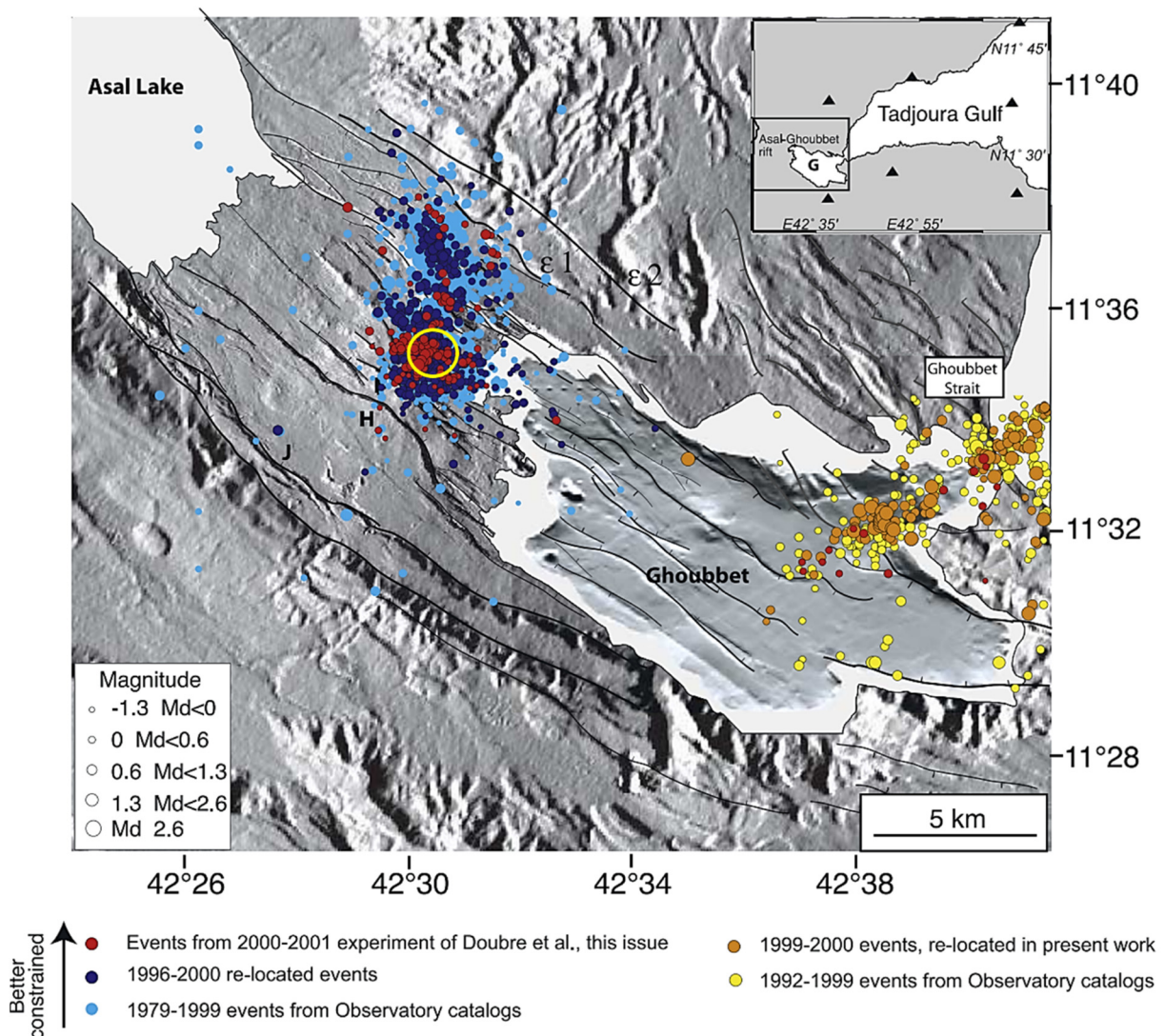


FIGURE 3: Distribution of seismic events between 1979 and 2001 in all the Asal-Ghoubbet rift. Colours distinguish the various data sets. Faults are marked in grey and the Fiale caldera area is marked by yellow circle. The inset shows permanent seismological stations (triangles) in the Ghoubbet and Tadjoura Gulf regions. G stands for Ghoubbet (from Manighetti et al., 2001a and modified by Doubre et al., 2007)

### 3.2 Stratigraphy

In total, six deep wells have been drilled in the Asal-Ghoubbet rift between 1975 and 1987. The wells Asal 1, 2, 3, 4 and 6 are located in the south-western part of the rift and only Asal 5 is situated in the central part of the area near the Fiale caldera (Aquater, 1989). Their location is given in the map in Figure 4.

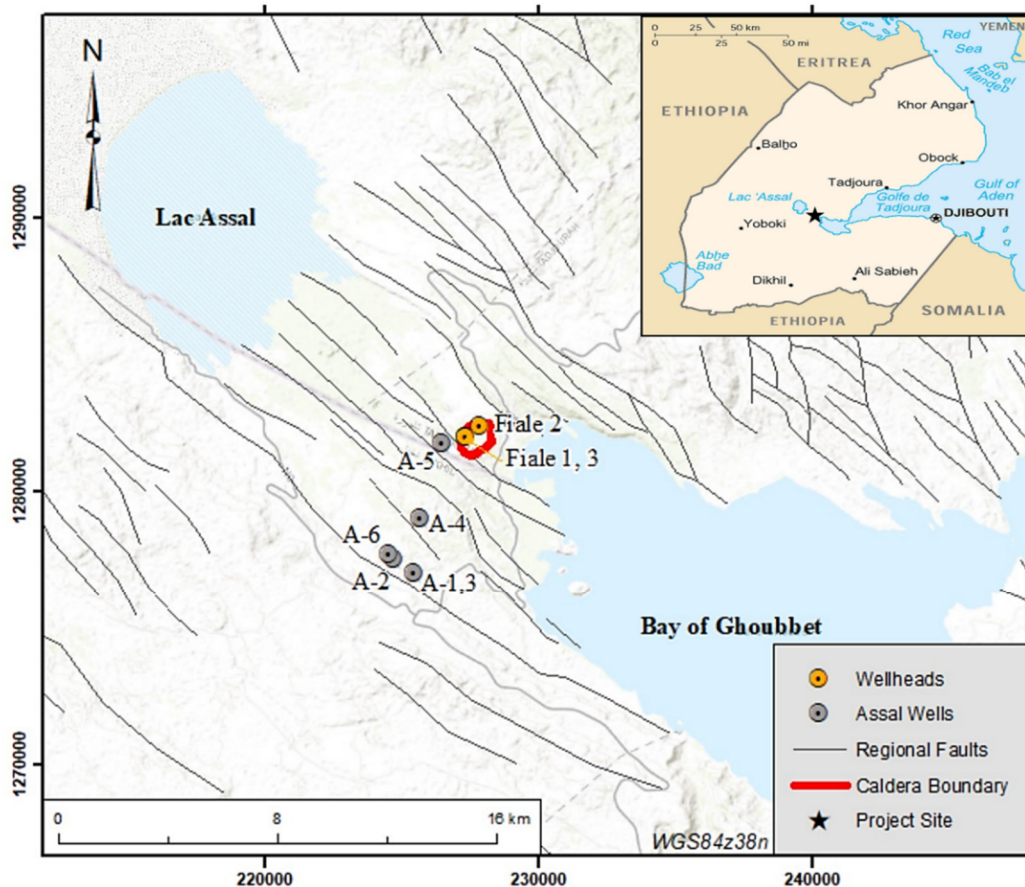


FIGURE 4: Location of Asal-Ghoubbet wells (from Le Gall et al., 2015)

The main stratigraphic units encountered in the wells Asal 1 to 6 from the top to the bottom are described below and illustrated in the SSW-NNE cross-section in Figure 5. The stratigraphy is based on ISERST (1985; 1986) and Barberi et al. (1975) and summarized by Aquater (1989).

*Asal series:* This unit comprises recent basaltic lava flows and hyaloclastites generated at the onset of the volcanism of the Asal rift with a maximum age of 1.05 Ma. The unit can further be divided into the “Série des Marges Externes d’Asal”, outcropping on both sides of the rift and the “Série de la Zone Centrale d’ Asal” outcropping on a 3-4 km wide belt in the inner part of the Asal rift.

*Afar stratoid series:* This unit overlies unconformably the Dalha basalt series. The volcanism of the central Afar produced a sequence of basalt-dominated fissure flows that are associated with rhyolitic volcanic centres. The different products found in this unit are mainly basaltic with intercalation of more evolved products such as trachytes, and rhyolites. Lacustrine deposits are also found. The age ranges between 4 and 1 Ma.

*Dalha basalts series:* This unit is formed by a sequence of basaltic lava flows intercalated with rhyolites, trachytes and detritic deposits. The reservoir zones were located in this unit in the wells Asal 1, 3 and 6. The age of the Dalha basalt series ranges between 8.9 and 3.8 Ma.

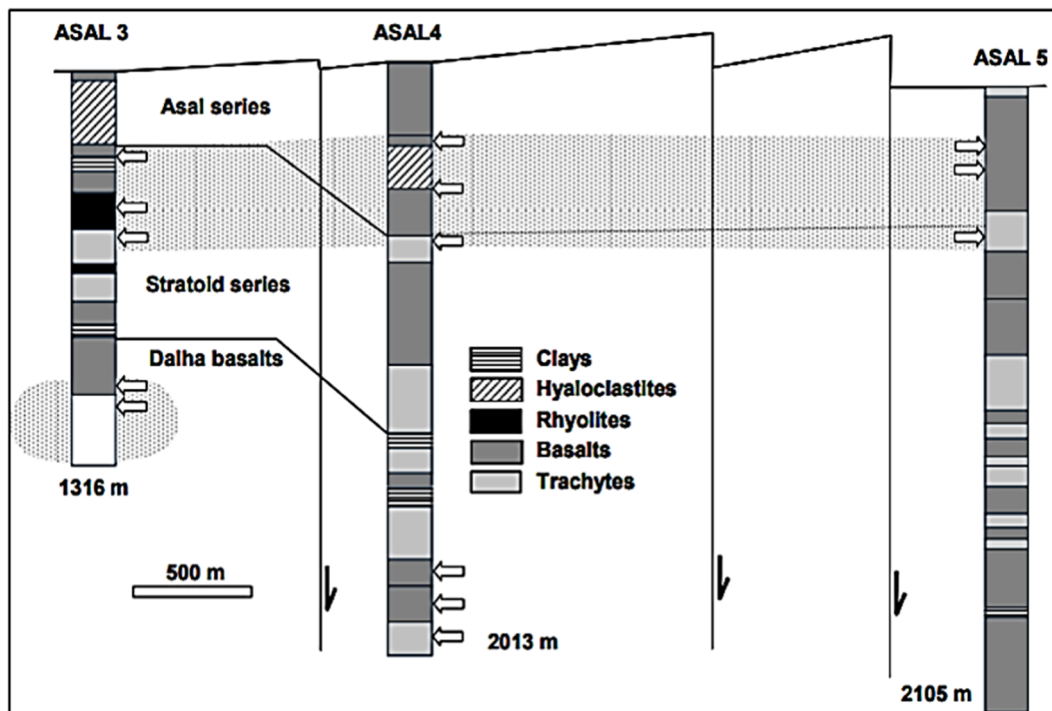


FIGURE 5: SSW-NNE cross-section through the south-eastern part of the Asal-Ghoubbet rift. The cross-section shows the stratigraphy of well A-3, A-4 and A-5 in the Gale-Le-Koma and Fiale geothermal fields as well as the drilled aquifers and the main faults within the explored area (from Aquater, 1989)

### 3.3 Pre-drilling conceptual model

A conceptual model for Asal rift area has been proposed by ÍSOR for ODDEG in December 2017 (Thorbjörnsson et al., 2017). The setting of this conceptual model is based on the previous and complete studies undertaken in the area, which is considered to have a viable geothermal potential. The data review included geological, geochemical, geophysical, hydrological and other available geoscientific data and interpretations.

In November 2017, geochemical analyses of seven springs in Asal NW at the border of the Asal Lake was carried out by ÍSOR and ODDEG. The chemical composition shows that it is mainly seawater of the Ghoubbet bay mixed with geothermal water that is on its way along the major NW-SE rift faults and/or has been heated up due to a high geothermal gradient. However, the high silica content in the spring water suggests mixing with geothermal fluids from the Fiale and/or Gale-Le-Koma reservoirs before flowing towards the Asal Lake (Thorbjörnsson et al., 2017).

Several geophysical studies have been undertaken in the area. According to Demange and Puvilland (1990), the low gravity anomalies in the residual Bouguer map correspond to the hyaloclastite volcanic formations found in the south- and north-western and south-eastern part of the rift. The high gravity values are mostly located in the inner part of the rift around the Lava Lake due to dense subaerial lava flows and/or dense intrusions at depth in the volcanic centre. The geophysical studies undertaken by Árnason et al. (1988, 2008) described high near-surface resistivity due to the fresh dry rocks above the groundwater table in the northwest part of the rift. Low resistivity is observed southeast of a hydrological barrier perpendicular to the rift in SW-NE direction (Figure 6). The smectite layer (clay cap), characterized by low resistivity, is found at different depths in the Asal rift. A high resistivity layer below the cap rock might be formed by the precipitation of high temperature alteration minerals such as the chlorite and epidote or a decrease in porosity. Finally, another low resistivity zone was detected below the high resistivity. Geothermal activity linked to hypersaline fluid could be the cause.



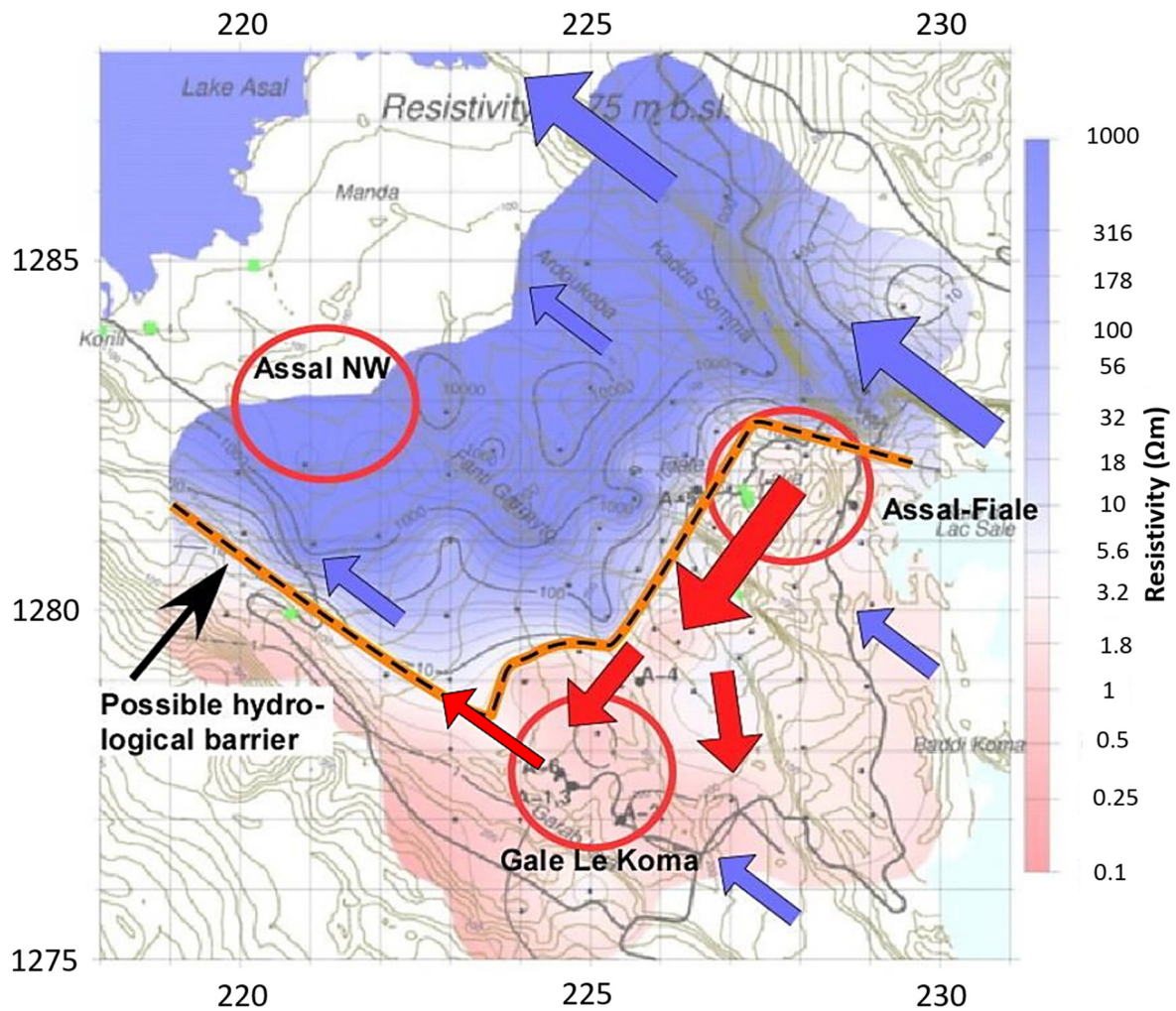


FIGURE 6: Hydrological barrier observed in the resistivity model at 75 m below the sea level (m b.s.l.). Hot flow under the Lava Lake flows along leaky transform zones described by Khodayar (2008) in S and SW direction. The hydrological barrier is indicated by an orange/black dotted line. Red and blue arrows show proposed movements of hot and cold water along the major NW-SE fault zones at 100-200 m depth and 500-800 m depth (taken from Árnason et al. 2008)

Árnason et al. (2008) proposed a first conceptual model of the Asal-Ghoubbet rift area based on the geophysical results (Figure 7). It consists to three distinct geothermal systems, which are Gale-Le-Koma in the SW, Asal-Fiale in the central part of the rift that includes the Fiale caldera and the Lava Lake, and Asal NW. The system under the Lava Lake shows more active heat mining than Gale-Le-Koma and the formation of a convective geothermal system due to the heating of cold seawater by the hot magma intrusions at depth. The heated seawater moves upwards under the Lava Lake and the precipitation of secondary minerals creates a hydrological boundary around the upflow zone. The seismic activity induced by the active rifting may open this barrier and allow the geothermal fluid to escape along the fractures. Indeed, the well Asal 5, located in Fiale caldera area, has a relatively high temperature (180°C) above 500 m. A lateral outflow of hot brine from the Lava Lake through the NNE-SSW trending faults (leaky transform zone) described by Khodayar (2008) might be the origin. However, the temperature drops to 80°C at 1000 m depth before rising to 350°C at 2100 m depth. The cooling could be explained by the inflow of cold seawater at 500 m depth through the major NW-SE faults in the Asal-Ghoubbet rift.

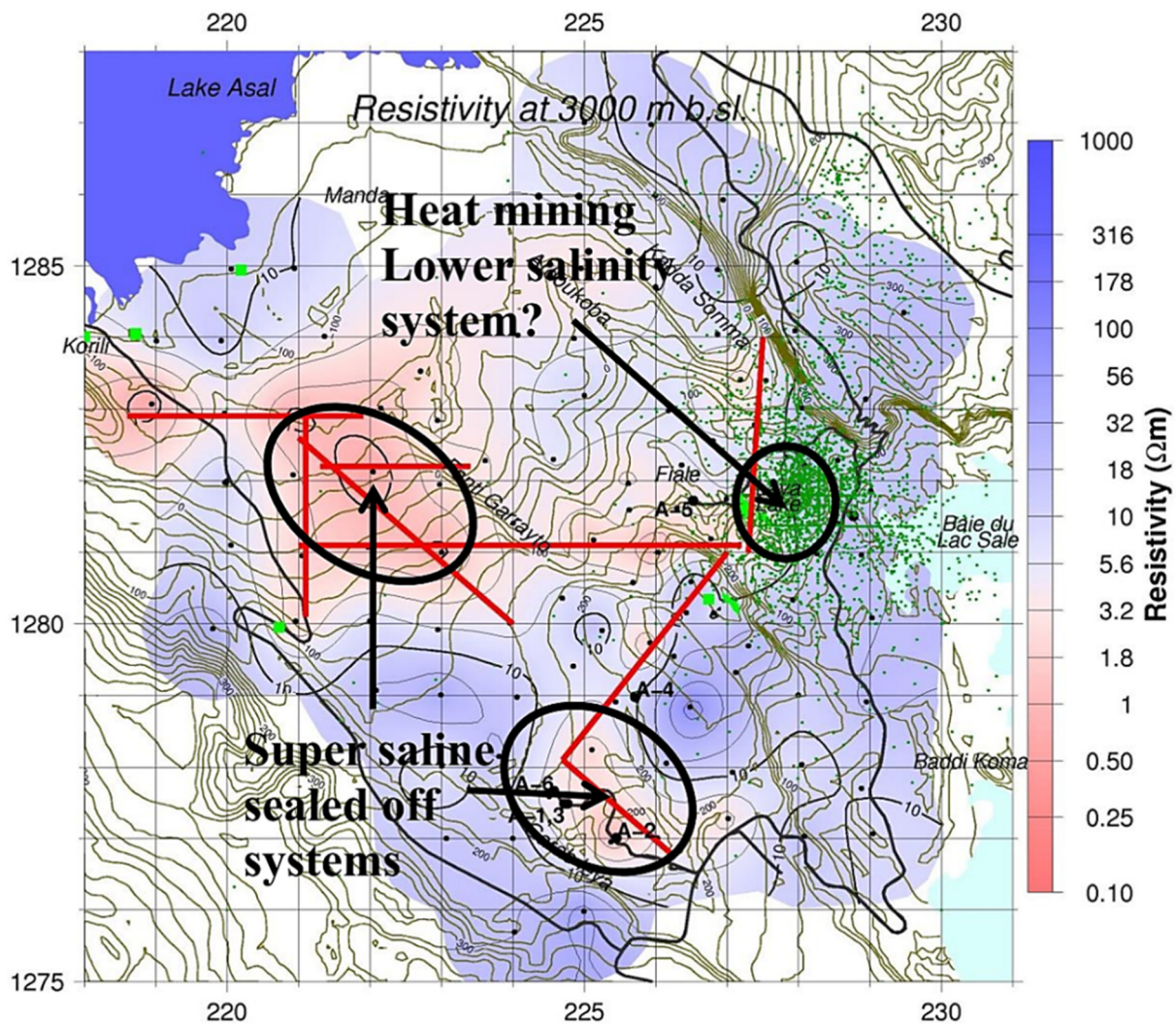


FIGURE 7: Conceptual model of geothermal activity in the Asal-Ghoubbet rift (taken from Árnason et al., 2008). The figure shows resistivity at 3000 m b.s.l., inferred lineaments of low resistivity (red lines), seismicity (dark green dots) and geothermal surface manifestations (light green). Two main geothermal systems sealed off and super saline are observed, and a more open lower salinity system is located under Lava Lake

The conceptual model by Árnason et al. (2008) summarized several characteristics/elements of the geothermal system in the Asal-Fiale zone. They are described below:

*Origin of the geothermal fluid:* Chemical and isotopic analyses suggest that seawater from the Ghoubbet basin is the origin of the geothermal fluids. However, the geothermal liquid is of high salinity due to boiling within the system. Moreover, the cold seawater which is rich in sulphate heats up and leads to the precipitation of anhydrite. Thus, anhydrite might fill the boundaries and decrease the permeability within the reservoir and between the surrounding geothermal systems. Indeed, these boundaries are shown in the resistivity model and are observed between the Fiale/Lava Lake area and Lake Asal trending NNE-SSW. These hydrological boundaries limit the flow at shallow depths between the Asal-Fiale/Gale-Le-Koma systems and Lake Asal (Árnason et al., 2008).

*Size of the geothermal system:* The difference in salinity and the possible presence of a hydrological barrier suggest a limited hydrological connection between the Gale-Le-Koma and Asal-Fiale geothermal systems on the one hand and Asal Northwest on the other.



*Boundary conditions:* Well Asal 5 in the Fiale caldera area does not show clay beds such as found in Gale-Le-Koma between 400 m and 600 m depth. Thus, hydrothermal alteration minerals (i.e. smectite) might control the shallow boundaries. The flow of water in the system might be limited by the active major faults trending in NW-SE direction. The vertical barriers around Asal-Fiale and Gale-Le-Koma are probably sealed by anhydrite and other alteration minerals. Finally, the lower boundaries are controlled by the hot brittle/ductile intrusions at 4-5 km depth as seen in Figure 8 (Árnason et al., 2008).

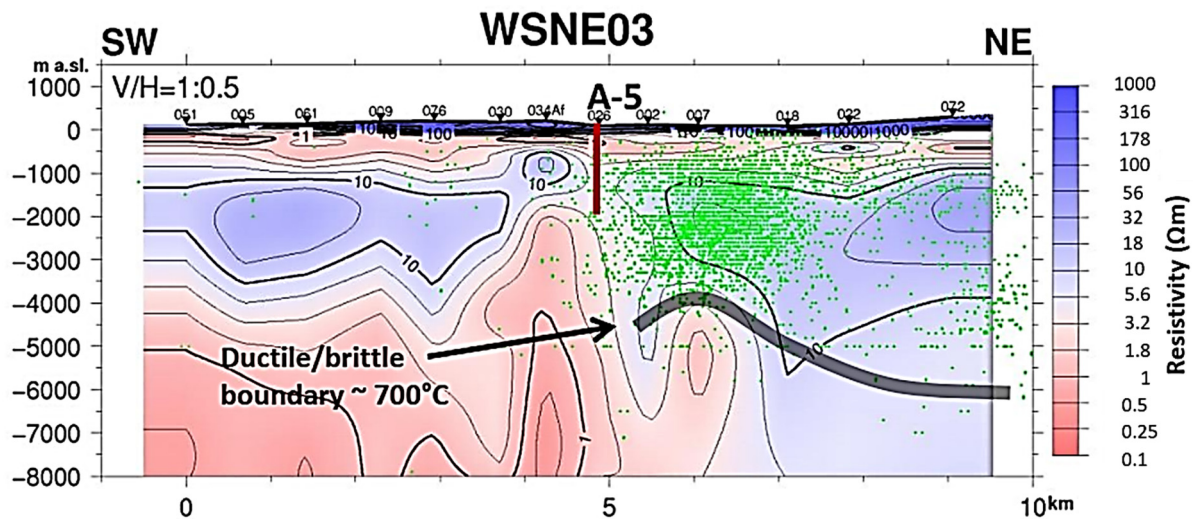


FIGURE 8: Resistivity cross-section across the Asal-Ghoubbet rift and location of earthquakes projected on the section. The estimated brittle/ductile boundary is indicated as a grey line below the deepest earthquakes. The maximum hypocentre depth domes up below the Lava Lake, indicating a heat source below the Lava Lake (from Árnason et al., 2008)

*Heat source:* The seismic studies show that there is no shallow magma chamber under Fiale/Lava Lake. Instead, the heat source in the Asal-Fiale system might be a combination of a high thermal gradient due to crustal thinning and hot intrusions at depth. Magma bodies might be located at greater depth than 5-6 km. In that case, the brittle/ductile boundary pointed out previously, might prevent the escape of magmatic fluids from greater depth.

### 3.4 Drilling of the well Fiale 3

Well Fiale 3 is in the north-western part of the Fiale Caldera in the Lava Lake on well pad number 2. The geographical coordinates of the well are projected in UTM Zone 38N using WGS 84 datum. They are 1281976N and 227346.4E with an elevation of 109 m above sea level (m a.s.l.). The well was directionally drilled to a measured depth of 2660 m in a N224° direction and a maximum inclination of 30°. All depth values are referenced to the rig floor that is 7.8 m above the surface. The well was drilled from 6<sup>th</sup> January to 23<sup>th</sup> February 2019.

The Icelandic Drilling Company was in charge of the drilling of well Fiale 3 for “Electricité de Djibouti” (EDD), using the drill rig Týr. Drill cutting analysis and geothermal consultancy services were conducted by ÍSOR (Iceland GeoSurvey). The drilling was carried out in three phases (Figure 9).

During the pre-drilling phase a casing depth of 140 m was reached on 12<sup>th</sup> of January. The 18<sup>5/8</sup>" surface casing was set to a depth of 112.7 m. Drilling of phase 1 was launched on 16<sup>th</sup> of January and reached a depth of 555 m on 20<sup>th</sup> of January. The kick off point (KOP) of the well was set at 542 m. The maximal inclination is 30° with an azimuth of 224°. Then, the 13<sup>3/8</sup>" anchor casing was set to 551.9 m depth. Phase 2 started on 25<sup>th</sup> of January. A depth of 1733 m was reached on 7<sup>th</sup> of February. The 9<sup>5/8</sup>"



production casing was run downhole to 1730 m. Finally, drilling of phase 3 (7" perforated liner) started on 15<sup>th</sup> of February and reached a measured depth of 2660 m on 23<sup>rd</sup> of February 2019.

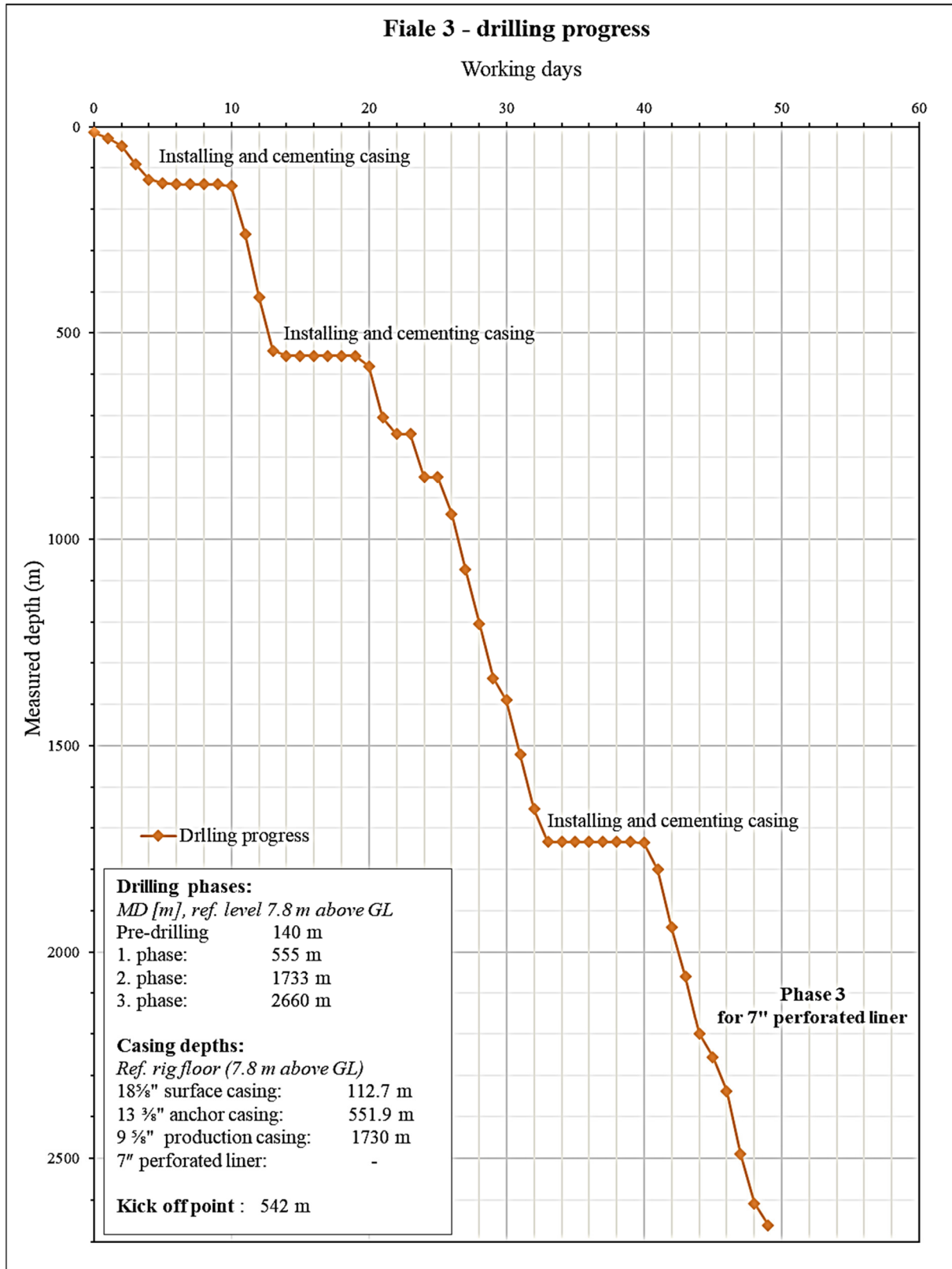


FIGURE 9: Drilling progress of well Fiale 3

#### 4. ANALYTICAL METHODS

This study is based on the rock cutting samples collected during the drilling of Fiale 3. The drill cuttings were sampled every 5 m from the surface to 555 m (MD) and every 3 m between 555 m and 2660 m (MD). Preliminary analysis using a binocular microscope was carried out at the rig site by the geologist. The first information obtained are the lithological composition and alteration mineralogy based on the physical or chemical properties of the minerals. These properties are the colour, crystal habit, texture, grain size, structure, effervescence in contact with diluted HCl and general composition of the rock. The vein fillings, evidence of intrusions, oxidation and alteration intensity are also noted. For further analysis, 48 samples were analysed in more detail in the ÍSOR laboratory to refine the lithology and alteration. The samples correspond to approximately 50 m intervals. For binocular analysis, an Olympus SX16 microscope was used.

The second analysis undertaken is the petrographic microscope analysis. In total, 11 thin sections were studied with the Leica DM 2700 P petrographic microscope at the ÍSOR laboratory. The epoxy used for the thin sections was stained blue in order to make the porosity easier visible. The objective is to identify and confirm the rock type previously obtained during binocular analysis, and to determine the hydrothermal alteration minerals and their paragenetic sequences as observed in veins and vesicle fillings. In this study, the main goal is to focus on the effect of the temperature reversal from 700 m to 1700 m (MWD).

The methylene blue absorption test is a reliable and simple method to obtain information about the presence of clay minerals in soils and rock cuttings. Helpful in the early stages of drilling, the amount of methylene blue adsorbed by the rock sample indicate the presence of swelling clay minerals (Verhoef, 1992). The total absorbed amount permits to calculate the methylene blue value and the cation-exchange capacity (CEC) of the rock. This simple and quick method has been used on the rig site to analyse smectite samples approximately every 20 m. The results, summarized in Appendix I, helped to delineate the interval depth of the smectite zone in combination with XRD analysis.

The X-ray diffractometer (XRD) is an instrumental technique used to identify fine-grained clays and other crystalline materials that are not easily identified with other techniques. It is a basic technique for clay mineral analysis (Moore and Reynolds, 1989). In the clay analysis, eight rock cuttings samples were chosen from depths of interest. The results are presented in Appendix II.

#### 5. RESULTS

##### 5.1. Lithostratigraphy

The lithology and alteration history of the well Fiale 3 is the result of two methods which are based on the binocular and petrographic microscopy techniques. The lithological log, shown in Figure 10, is dominantly based on the rock cuttings analysis undertaken on the rig site during the drilling of the well. The thin section analysis helped to verify the rock type and to analyse the alteration minerals assemblage in the depths of interest. The lithological formations are dominantly formed by the alternation of basaltic lavas and intermediates rocks. Acidic rocks are identified at the lowermost part of Fiale 3. The formations were divided into four main stratigraphic units which are the Asal series (0-440 m), the Afar stratoid series (440-1022 m), the Dalha basalt series (1022-2240 m) and the Mabla rhyolite (2240-2660 m). The description of these rock units is presented below.

*14.4-20 m, no formation:* Mixed fragments of sand, gravel and wood chippings.

*20-25 m, basalt:* Grey, medium-grained basaltic lava, crystalline with large and elongated phenocryst of plagioclase. The rock is relatively fresh.

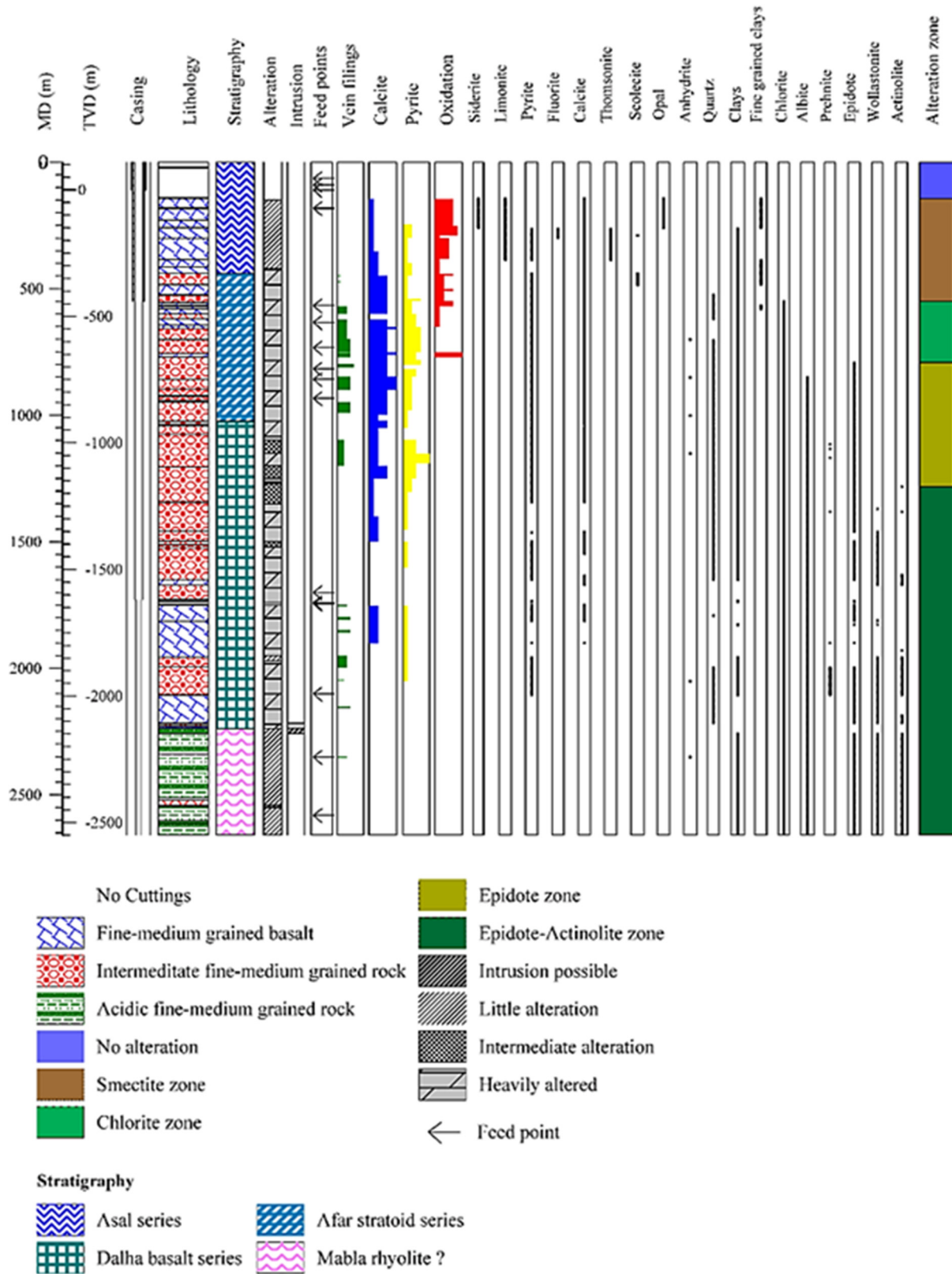


FIGURE 10: Distribution of lithology and alteration minerals in Fiale 3

25-140 m, no cuttings: Total loss of circulation.

140-143.8 m, no formation: Sweep sample, mixed fragments of cement and basaltic materials.



143.8-180 m, *basalt*: Grey to pale brown, fine- to medium-grained rock. It is porphyritic with phenocrysts of plagioclase and quartz. The formation is mixed with vesicular fragments (scoria). It is moderately oxidized. Fine-grained clays, opal and limonite are noted in the vesicles. Other secondary minerals include calcite and siderite. Minimal alteration intensity.

180-185 m, *no cuttings*

185-260 m, *basalt*: Same as the formation between 143.8-180 m. The difference is an increase of oxidation.

260-300 m, *basalt*: Dark grey, fine- to medium-grained rock moderately porphyritic with plagioclase and quartz phenocryst. Fine-grained clays and fluorite fill the vesicles. Limonite is noted lining vesicle walls at 285 m. Cluster of scolecite observed at 290 m. Pyrite disseminated in the rock matrix. Secondary minerals include clays, calcite, limonite, pyrite, fluorite, thomsonite and scolecite. Minimal degree of alteration.

300-385 m, *basalt*: Brown, fine- to medium-grained rock moderately vesicular. Phenocryst of plagioclase and quartz are found. Vesicles filled by clays and calcite. Calcite is the result of replacement of primary minerals such as plagioclase, the ferromagnesian minerals (pyroxene and olivine) and glass in the groundmass. Moderately oxidized and slight degree of alteration. Secondary minerals include calcite, clays, limonite, thomsonite and pyrite.

385-440 m, *basalt*: Fine- to medium-grained rock, dark grey in colour with large phenocryst of plagioclase. Calcite found frequently in the groundmass, in vesicles, and in veins at 430 m. Secondary minerals include calcite, clays, limonite, and pyrite. Less oxidized. Minimal degree of alteration to moderate at the bottom of this unit.

440-485 m, *intermediate rock*: Grey fine- to medium-grained rock with phenocryst of plagioclase, quartz and K-feldspar (sanidine). Slightly vesicular with infills of calcite, fine-grained clays and scolecite. The rock is moderately oxidized (440-450 m) at the contact with the overlying basaltic formation. Pyrite veins at 480 m but also found in groundmass. A general increase in calcite levels within this depth interval. Secondary minerals include clays, calcite, scolecite, fluorite and pyrite. Little to moderate alteration.

485-525 m, *basalt*: Dark grey to pale brown, fine- to medium-grained vesicular with plagioclase and quartz phenocrysts. Vesicles are largely infilled by calcite and both fine-grained green and brown clays. Calcite, clays and pyrite are noted as secondary minerals. Little to moderate alteration.

525-555 m, *intermediate rock*: Fine- to medium-grained rock, pale grey in colour. Elongated and striated sanidine phenocrysts. Vesicles infilled by secondary quartz, calcite and fine-grained clays. Some basaltic fragments are found mixed with the sample. The rock is relatively dense and lightly to moderately altered. Calcite, clays, secondary quartz and pyrite are noted as secondary minerals.

555-566 m, *basalt*: Grey to pale brown, fine- to medium-grained porphyritic rock with plagioclase and occasional quartz phenocrysts. Calcite and fine-grained clays replace both the groundmass and plagioclase phenocrysts. The formation is slightly fractured and depicts moderate degree of oxidation. Alteration degree is low to medium with pyrite disseminated in the rock matrix. Secondary minerals include clays, pyrite, calcite, and secondary quartz.

566-569 m, *no cuttings*

569-600 m, *basalt*: Fine-grained porphyritic rock with mainly phenocryst of plagioclase. Grey in colour. Vesicles infilled by secondary quartz, calcite, fine-grained clays and some white nodular mineral. Most of the phenocrysts have been replaced by coarse grained green clays and calcite. The rock is fractured and pyritization is noted. Oxidation is also observed. Secondary minerals include clays, pyrite, calcite and secondary quartz. Low to medium alteration.

600-620 m, *intermediate rock*: Pale grey, fine-grained rock with plagioclase, sanidine and quartz phenocrysts. The vesicles are filled by calcite, coarse grained clays and euhedral secondary quartz. At

605 m and 608 m green coarse-grained clays are observed on the rim with secondary quartz growing on the core. Mixed with basaltic fragments between 614-620m. Moderately altered with pyrite disseminations in the rock matrix. Secondary minerals include clays, calcite, pyrite and secondary quartz.

*620-644 m, basalt:* Fine-grained rock, pale grey in colour with rare phenocryst of plagioclase. Veins of clays, pyrite, and calcite are noted. Pyrite and calcite are also found in the groundmass replacing mafic minerals and plagioclase. Secondary minerals include clays, calcite and pyrite. Low to medium alteration degree.

*644-656 m, basalt:* Pale grey to pale green, fine-grained rock with plagioclase phenocrysts. Calcite, coarse grained clays and secondary quartz fill the vesicles. Moderately altered with pyrite in the matrix.

*656-756 m, intermediate rock:* Pale to grey, fine- to medium-grained rock with plagioclase, sanidine phenocrysts and minor primary quartz. The rock shows a trachytic texture where primary feldspar is aligned in a flow direction. Calcite and clays are filling the vesicles. Pyrite, secondary quartz and calcite are found in veins. At 700 m, albite and anhydrite are found and observed under the petrographic microscope. The occurrence of anhydrite indicates the presence of seawater in the well at the time of the formation. Moderately altered.

*756-771 m, basalt:* Brown fine-grained rock. At 759 m the cuttings are mixed with abundant fragments of scoria and intermediate rock. Clay minerals and calcite fill the vesicles. Alteration minerals are quartz, calcite, clays, minor pyrite, albite, and anhydrite.

*771-923 m, intermediate rock:* Grey to pale grey in colour, fine-grained rock with anhedral sanidine. Veins filled with calcite, coarse-grained clays and quartz are common. Epidote occurs at 792 m in association with quartz and with prehnite at 798 m. Different paragenetic sequences are observed such as quartz-epidote in veins at 813 m, epidote overgrowing calcite at 899 m, coarse-grained clay minerals and epidote at 902 m. Veins of quartz, calcite-pyrite, pyrite-epidote are observed along this interval. High albitization of feldspar minerals is also noted in the thin sections. The degree of alteration has highly increased. Secondary minerals are clays, pyrite, prehnite, epidote, quartz, and albite.

*923-926 m, basalt:* Grey fine- to medium-grained rock with large phenocryst of plagioclase. The cuttings appear massive with low to medium alteration. Less pyrite, epidote and calcite in veins are observed.

*926-944 m, intermediate rock:* Fine- to medium-grained rock with grey colour is medium to highly altered. Primary minerals observed are sanidine phenocryst. Clay minerals fill the vesicles. The sample is mixed with dark grey fragments of rocks relatively fresh and massive. Secondary minerals are epidote, quartz, clays, pyrite, calcite, albite.

*944-950 m, basalt:* Same as 923-926 m.

*950-1022 m, intermediate rock:* Same as 926-944 m but not mixed with dark brown fragments. High occurrence of epidote noted at 992 to 1001 m and the amount of pyrite has decreased. Veins are common at 977 m to 983 m. Petrographic analysis showed albite which formed replacing primary feldspar in a process called albitization. Anhydrite is also observed at 1001 m.

*1022-1025 m, acidic rock:* Pale grey to colourless felsic rock. It is glassy, quartz rich. Minimal alteration intensity.

*1025-1037 m, intermediate rock:* Same as 950-1022 m.

*1037-1043 m, acidic rock:* Same as 1022-1025 m but veining of epidote and pyrite are observed.

*1043-1076 m, intermediate rock:* Same as 926-944 m but with medium to high intensity of alteration.

*1076-1205, intermediate rock:* Same as 1043-1076 m with high alteration degree. Epidote is more abundant, pyrite has decreased. Prehnite is observed in association with epidote at 1133 m. Mineral evolution sequences are common and are observed as follows: quartz-epidote at 1085 m, 1166 m and

1172 m, course grained clays-prehnite at 1115 m, course grained clays-epidote at 1127 m and 1151 m, and quartz- prehnite at 1169 m. Albite and anhydrite crystals are observed in thin sections.

*1205-1344 m, intermediate rock:* Same as 1076-1205 m with higher degree of alteration. Calcite and pyrite have decreased. Epidote is more abundant and actinolite is first observed at 1283 m.

*1344-1458 m, intermediate rock:* Pale grey intermediate rock. Aphyric with K-feldspars and subordinate plagioclase. Pyrite and calcite are found in small amount. Wollastonite is first observed at 1371 m as white fibrous mineral. Low- to high-temperature paragenetic sequences of clays-prehnite and epidote-actinolite were observed at 1383 m. Other minerals are epidote, clays, prehnite, quartz, pyrite, albite, and calcite. Medium to high alteration degree.

*1458-1497 m, intermediate rock:* Pale grey, fine- to medium-grained rock. It appears massive and moderately altered. Very low amount of calcite and pyrite. Epidote and quartz are observed in association. Wollastonite and coarse-grained clays are present.

*1497-1512 m, intermediate rock:* Pale grey to pale green fine-grained rock highly altered. Wollastonite, epidote, clays, quartz, calcite and pyrite (rare) are observed.

*1512-1524 m, intermediate rock:* Same as 1458-1497 m.

*1524-1650 m, intermediate rock:* Grey fine-grained rock moderately porphyritic with sanidine moderately altered. Epidote still abundant, actinolite is common between 1632-1671 m. Quartz, clays, wollastonite and pyrite are observed.

*1650-1671 m, basaltic rock:* Grey fine- to medium-grained rock with phenocrysts of plagioclase and sanidines. Moderately altered with occurrence of actinolite and wollastonite.

*1671-1728 m, intermediate rock:* Same as 1524-1650 with wollastonite more abundant. Crystal intergrowth of wollastonite and epidote is also common between 1701 m to 1725 m.

*1728-1733 m, no cuttings.*

*1733-1736 m, mix of cuttings fine- to medium-grained highly altered rock.* It is a mixture of basalt, metal chippings and intermediate rock. The rock grains are highly altered. Epidote occurrence is high in the rock mixture. Well-formed cubes of pyrite and coarse-grained clays are also observed.

*1736-1749 m: no cuttings*

*1749-1813 m, basalt:* Fine- to medium-grained dark grey rock shows veins of epidote with quartz in association. Fragments of cement and reddish grains are observed. Pyrite and calcite occur in traces. Wollastonite and clays are found. High alteration degree.

*1813-1957 m, basalt:* Grey fine- to medium-grained rock with phenocrysts of plagioclase and minor sanidine and mixed with grey intermediate rock, which appear less altered. The rock seems to be coarser grained at 1900 m. Wollastonite, epidote, clays, actinolite, albite are observed. Pyrite and calcite still in traces.

*1957-2105 m, intermediate rock:* Grey to light grey fine-grained rock with medium to high alteration. Different association of minerals are noted such as quartz-actinolite, epidote-wollastonite, and epidote-quartz in veins. Wollastonite, pyrite, clays, prehnite, coarse-grained clay minerals, epidote, actinolite, and quartz are observed. Anhydrite is found again at 2050 m.

*2105-2216 m, basalt:* Grey fine-medium rock moderately altered. Wollastonite, clays, epidote, pyrite in traces, actinolite, and quartz are observed.

*2216-2219 m, acidic rock:* Whitish, felsic, holocrystalline, fine-medium grained rock with high content of quartz sanidine. Low alteration.

*2219-2228 m, intermediate rock:* Pale grey moderately aphyric with sanidines and minor plagioclases. K-feldspars are common. Alteration mineralogy has reduced. Occurrence of clays has also reduced. The rock is less altered than between 2216-2219 m.

2228-2237 m, *basalt*: Dark grey medium- to coarse-grained lava. Phenocrysts of plagioclase are observed in the groundmass. The rock shows little alteration.

2237-2258 m, *acidic rock*: Same as 2216-2219 m.

2258-2339 m, *acidic rock*: Fine-grained to glassy rock, light grey in colour. The rock is rich in plagioclase and quartz phenocrysts that appear dark grey. The rock shows medium alteration. However, high-temperature alteration minerals are observed such as epidote, wollastonite, actinolite, and clays in smaller amounts. Magnetite is abundant.

2339-2512 m, *acidic rock*: Same as 2258-2339 m but grey in colour.

2512-2543 m, *intermediate rock*: Light grey rock rich in k-feldspars moderately phyrical with phenocrysts of sanidine, darker quartz and plagioclase. The degree of alteration is high. Alteration minerals include wollastonite, actinolite, epidote and clays. Magnetite is abundant.

2543-2603 m, *acidic rock*: Same as 2258-2339 m. Anhydrite is found at 2351 m.

2603-2615 m, *acidic rock*: Light grey to whitish fine- to medium-grained holocrystalline quartz-rich rock. It is massive and shows low alteration.

2615-2660 m, *acidic rock*: Same as 2258-2339 m. Fine-grained to glassy rock, light grey in colour. The rock is rich in plagioclase and quartz phenocrysts that appear dark grey. The rock shows medium alteration.

## 5.2 Hydrothermal alterations

### 5.2.1 Alteration of primary minerals

Hydrothermal alteration is the interaction of the host rocks with the hot water and steam that leads to the dissolution of primary minerals and the deposition of secondary minerals by replacement and precipitation (Henley and Ellis, 1983). Several factors influence the degree of alteration such as the permeability, the temperature, the rock type, the hydrothermal fluid composition, the duration of the water-rock interaction, the number of superimposed hydrothermal regime, and the hydrological parameters (Kristmannsdóttir, 1976). Changes in the hydrothermal environment lead to the precipitation of secondary minerals in open spaces such as cavities, vesicles and fractures in the rocks. The primary minerals in the groundmass are also replaced by secondary minerals.

The primary minerals in well Fiale 3 include mainly feldspars (plagioclase and K-feldspar), pyroxene, opaque minerals, very rare quartz, olivine and glass, whereof olivine and glass show high degree of alteration. Primary minerals which form at high temperature show little resistance to hydrothermal alteration (Stefánsson et al., 2001). The alteration of primary minerals is described below and summarized in Table 1.

*Volcanic glass* is the most unstable phase and the first to be altered. In well Fiale 3 glass has been very rare. It alters to clays, calcite, and quartz.

*Olivine* is a magnesium-iron silicate. This primary mineral crystallizes rapidly during the cooling of the magma. It is also the first to alter. In this case, olivine was rarely observed below 300 m depth (MD) and has been altered into oxides in the shallower part. It can also be replaced by pyrite, chlorite and other green clays if magnesium is present.

*Pyroxene* is the most significant and abundant group forming ferromagnesian silicates and is one of the main primary minerals observed in Fiale 3. It appears as small phenocrysts in the groundmass and individual large euhedral phenocrysts of clinopyroxene. It shows different rate of alteration in the



TABLE 1: Alteration of primary minerals based on petrographic and XRD analyses

Depth	Rock	Primary minerals	Alteration degree	Alteration minerals
300	Basalt	Volcanic glass	XXX	Sm, Cal
		Olivine	XXX	Sm, Cal
		Pyroxene	X	Sm
		Feldspars		
		Opaque minerals	XX	Py, Lm
450	Intermediate rock	Volcanic glass	XXX	Sm, Cal
		Olivine	XXX	Sm, Cal
		Pyroxene	X	Sm, Cal
		Feldspars	X	Sm, Cal
		Opaque minerals	XX	Py, Lm
700	Intermediate rock	Volcanic glass	XXX	Clays, Cal
		Olivine	XXX	Clay, MLC, Cal
		Pyroxene	X	Cal, Chl
		Feldspars	XX	Cal, Qz, Chl
		Opaque minerals	XX	Py
851	Intermediate rock	Volcanic glass	XXX	Clays, Cal
		Olivine	XXX	Clays, Cal
		Pyroxene	X	Cal, Chl
		Feldspars	XXX	Clays, Cal, Qz, Chl, Ab, Ep
		Opaque minerals	XX	Py
1001	Intermediate rock	Volcanic glass	XXX	Clays, Cal
		Olivine	XXX	Clays, Cal
		Pyroxene	XX	Chl, Ep
		Feldspars	XX	Cal, Qz, Chl, Ab, Ep
		Opaque minerals	X	Py
1151	Intermediate rock	Volcanic glass	XXX	Clays, Cal
		Olivine	XXX	Clays, Cal
		Pyroxene	XX	Chl, Ep
		Feldspars	XX	Cal, Qz, Chl, Ab, Ep
		Opaque minerals	X	Py
1302	Intermediate rock	Volcanic glass	XXX	Clays, Cal
		Olivine	XXX	Clays, Cal
		Pyroxene	XX	Chl, Ep, Act
		Feldspars	XXX	Cal, Qz, Chl, Ab, Ep, Act
		Opaque minerals	X	Py
1449	Intermediate rock	Volcanic glass	XXX	Clays, Cal
		Olivine	XXX	Clays, Cal
		Pyroxene	XX	Chl, Ep, Act
		Feldspars	XX	Cal, Qz, Chl, Ab, Ep, Act, Wo
		Opaque minerals	X	Py
1900	Basalt	Volcanic glass	XXX	Clays, Cal
		Olivine	XXX	Clays, Cal
		Pyroxene	XX	Chl, Ep, Act
		Feldspars	XX	Cal, Qz, Chl, Ab, Ep, Act, Wo
		Opaque minerals		
2050	Intermediate rock	Volcanic glass	XXX	Clays, Cal
		Olivine	XXX	Clays, Cal
		Pyroxene	XX	Chl, Ep, Act
		Feldspars	XX	Qz, Chl, Ab, Ep, Act, Wo
		Opaque minerals		
2351	Acidic rock	Pyroxene	XX	Chl, Ep, Act
		Feldspars	XXX	Qz, Chl, Ab, Ep, Act, Wo

**Key:** Sm: Smectite; Cal: Calcite; Lm: Limonite; Py: Pyrite; MLC: Mixed layer clay; Qz: Quartz; Chl: Chlorite; Ab: Albite; Ep: Epidote; Act: Actinolite; Wo: Wollastonite;  
**Alteration degree:** X: slightly altered; XX: medium altered; XXX: highly altered

petrographic analysis. At 2050 m and 2351 m, the large crystals show a lower alteration degree. It alters into clays but also into epidote and actinolite.

*Feldspars* minerals are the most abundant in igneous rocks. Plagioclase has been found in the different formations of the well as described previously. It appears colourless to white, flat, columnar or granular and shows a parallel cleavage under the binocular microscope. It is identified by its low relief and polysynthetic twinning under the petrographic microscope. It occurs as fine in the groundmass but also large in rocks exhibiting porphyritic textures. Fresh in the upper part, it traps fluid inclusions along their twinning. It is fractured and clay minerals are formed along the fractures. It alters into albite, epidote, calcite, and secondary quartz. Potassium feldspars are also observed in the evolved formations such as intermediate and acidic rocks. Sanidine is very common and is readily identified by its low relief, weak birefringence and simple twinning. Less observed microcline is found at 1001 m, 1302 m, and 1449 m. It is relatively fresh but can give the same alteration products.

*Opaque minerals* occur all along the well in different amounts. Magnetite is isotropic and appears opaque under petrographic microscope. It is present in major amounts in the deepest formations.

*Quartz* occurs regularly in the rock. However, most of the quartz seems to be formed during secondary processes.

### 5.2.2 Distribution of alteration minerals

The distribution and abundance of the hydrothermal minerals were obtained from the petrographic and binocular microscopy observations and XRD analyses. The main hydrothermal minerals in Fiale 3 are actinolite, albite, anhydrite, calcite, different type of clays, epidote, pyrite, and quartz. In addition, minor amounts of fluorite, prehnite, and zeolites such as scolecite, and thomsonite are found. Their distribution is summarized below.

*Oxides* are mainly iron oxides and form at the surface or in a near surface environment where oxygen-rich fluids interact with the rock. Oxidation is observed from the top of the well to 550 m depth. Limonite occurs. It forms by the oxidation of ferrous minerals such as magnetite observed in the ground mass.

*Pyrite* crystals are very common in the well from the shallower depth to down 1500 m. It becomes very rare between 1500 m and 1650 m. It is found again until 1800 m depth and from there on only in traces to the bottom of the well. It forms euhedral cubic crystals with brassy yellow metallic colour. In thin sections, it is opaque and with a granular form only observed in a reflected light. It appears as a replacement of opaque minerals disseminated in rock groundmass and infillings in open spaces such as fissures, veins and vesicles.

*Fluorite* is very rare. It occurs at two depth intervals, 260 to 300 m and 440 to 485 m depth. It was observed only during the cutting analysis. It forms cubes, octahedrons or spheres. It is colourless, greenish or pale violet.

*Calcite* is the most abundant alteration mineral observed continuously from 180 m depth to the bottom of the well. However, its amount varies, it is more present in the upper part and less in the deeper part. It is generally white with a vitreous lustre and appears granular. It effervesces in dilute hydrochloric acid. In thin section, calcite is recognized by its high birefringence, three perfect cleavages and twinkling relief upon rotation of the microscope stage. In general, it appears as a replacement mineral of plagioclase. It can also be found as deposit in vesicles and fractures forming sequences with clays, epidote, quartz and anhydrite.

*Zeolites* occur rarely in Fiale 3. They belong to a group of authigenic minerals which precipitate extensively from alkaline hot water in geothermal systems. Their occurrence depends mostly on the

temperature (Bird et al., 1984, Weisenberger and Selbakk, 2009, Spürgin et al., 2019). Most of them are low-temperature minerals characterized by deposition temperatures between 40 and 120°C. In this well zeolite minerals occur only rarely and were only identified during cuttings analysis. Thomsonite forms white dense masses of radiating crystals with spherical clusters filling vesicles. It was found in low amount between 260 m and 385 m. The second zeolite observed is scolecite. It forms colourless radial crystals and is found at 260-300 m and 440-485 m.

*Anhydrite* ( $\text{CaSO}_4$ ) forms when sulphate-rich seawater mixes with hot calcium-rich hydrothermal fluid or becomes insoluble when seawater is heated to temperatures above 150°C (Marks et al., 2010). In well Fiale 3, anhydrite occurs between 700 m and 1151 m under the petrographic microscope. It appears again at 2050 m and 2351 m. In thin section, it is colourless with a moderate positive relief in (plane-polarized light (PPL) and has a high birefringence in third order in cross-polarized light (XPL) (Figure 11). It occurs in aggregates of anhedral to blocky crystals at 1151 m and with epidote at 2050 m. It can also form euhedral elongated fibres. Its presence is explained by the large intrusion of cold seawater in the rift through the faults in direction of Lake Asal.

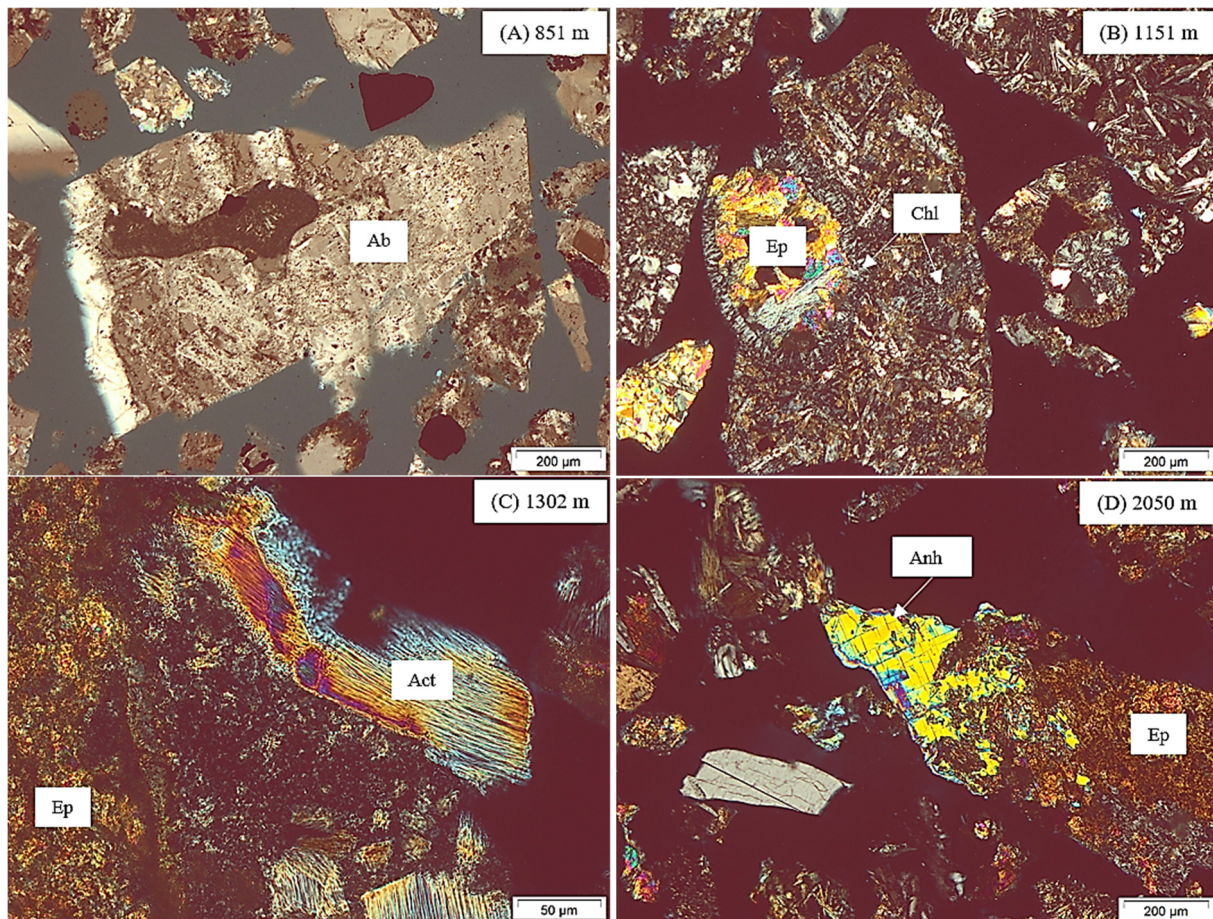


FIGURE 11: Thin section A shows Albite (Ab); B shows vesicle filled by chlorite (Chl) and epidote (Ep); C shows Actinolite (Act), and D shows an assemblage of epidote (Ep) and anhydrite (Anh)

*Quartz* is colourless to white in colour and occurs in euhedral to subhedral crystals. It is identified under the binocular microscope at 525 m depth. In thin section, it is found as infillings in fissures, vesicles, and rarely in veins. It can also appear as an aggregate of crystals. It is associated with other minerals such as calcite, pyrite, and epidote. Quartz forms at around 180°C.



*Clay minerals* are common and abundant alteration products in hydrothermal system. They are hydrous phyllosilicates and are found in both high- and low-temperature fields (Kristmannsdóttir and Tómasson, 1978). According to Ahmed (2008), the composition, morphology and structure of clays depend on different factors, such as host rocks, temperature, and fluid composition. The occurrence of clay minerals can help to interpret the thermal history of a geothermal system (Reyes, 2000). They have been identified by XRD, petrography and binocular analyses.

- *Smectite* is a low-temperature clay mineral occurring as replacement of primary minerals. XRD analyses and methylene blue test results show the presence of smectite between 145 and 550 m (MD). This corresponds to the clay cap rock.
- *Mixed layer clay (MLC)* has been found with chlorite at 700 m by XRD.
- *Chlorite* starts to form at an equilibrium temperature of 220°C. It was identified at 700 m with MLC by using XRD analyses. Its occurrence is observed to the bottom of the well.

*Albite* is the alteration product of primary K-feldspar and plagioclase phenocrysts replacement. With the increase of temperature, the process of albitization leads to the disappearance of the twinning of the feldspars and causes a cloudy appearance (Figure 11). Albite is noted from 851 m to the bottom. It forms at temperatures above 180°C.

*Epidote* occurs first at 792 m depth and stays abundant to the bottom of the well. It is yellowish-green in colour with a strong relief in PPL. It has a high birefringence with a yellow to green colour in XPL. First crystals are anhedral and form fine-grained aggregates and in deeper zones, they appear idiomorphic, tabular, radiated or fibrous. Epidote is found as replacement of primary feldspar and pyroxene but also as filling in veins and vesicles in association with, albite, quartz, chlorite, actinolite, calcite, and pyrite (Figure 11).

*Wollastonite* occurs as an aggregate of elongated fine radiating crystals with a typical white to grey colour. It is observed first at 1371 m. In thin sections, it is colourless to white with a low interference colour of first order grey. It is associated with epidote and anhydrite at 2050 m. Wollastonite indicates temperatures above 270°C.

*Actinolite* belongs to the amphibole group and is formed as a replacement of primary minerals such as pyroxene and plagioclase. It appears as green to pale-green radiating fibres and massive to granular aggregates in the groundmass and individual crystals. It was first observed at 1283 m under the binocular microscope and at 1302 m in thin sections (Figure 11). It is present in the rest of the well and is found in association with epidote, albite and chlorite. It indicates high temperatures above 280°C.

### 5.2.3 Alteration mineral zones

In Fiale 3, five alteration mineral zones have been identified. Each zone is marked by the first occurrence of a higher temperature alteration mineral, which is indicative of increasing temperatures. Based on the results of the binocular, petrographic and XRD analysis, the alteration zones are described below and summarized in Figure 10. The alteration zones indicate a prograde alteration system.

*Unaltered zone (0-145 m)*: The lithology in this interval consists of fresh basaltic lava flows slightly oxidized. This zone is also characterized by total losses of circulation.

*Smectite zone (145-550 m)*: This zone corresponds to the clay cap characterized by the presence of smectite clay. The mineral has been identified with the help of XRD and the methylene blue test. However, calcium sulphate minerals have been found at 450 and 550 m, possibly anhydrite, formed as a result of fresh seawater infiltration.

*Chlorite zone (550-792 m)*: This interval is defined by the occurrence of mainly unstable chlorite. At 700 m, a small peak of mixed layer clay is detected.

*Epidote zone (792-1283 m):* This zone is characterized by the first appearance of epidote at 792 m. Chlorite is also very common. Other alteration minerals include albite, quartz, and anhydrite.

*Epidote-Actinolite zone (1283-2660 m):* This zone is identified by the occurrence of actinolite at 1283 m. High-temperature alteration minerals are also common in this interval such as epidote, chlorite, wollastonite, albite, and quartz. Anhydrite is also observed in thin sections and at 1151 m in XRD analysis.

#### 5.2.4 Hydrothermal alteration mineral deposition sequence

According to Brown (1978), deposition of alteration minerals in open spaces such as vesicles, veins, vugs and fractures depends on various factors which are porosity, permeability, temperature, fluid composition, and the duration of the interactions. The study of the sequences of mineral deposition provides information about the processes involved, as well as the time scale and the temperature changes.

The observation of thin sections permits to determine and/or to confirm the different alteration minerals observed in the well Fiale 3. Their occurrence is summarized in Table 2.

TABLE 2: Occurrence of alteration minerals based on binocular, petrographic and XRD analysis

Depth m (MD*)	Alteration minerals									
	Cal	Py	Anh	Qz	MLC	Chl	Ab	Ep	Wo	Act
300	X	X								
450	X	X	X							
700	X	X	X	X	X	X	X			
851	X	X	X	X		X	X	X		
1001	X	X	X	X		X	X	X		
1151	X		X	X		X	X	X		
1302				X		X	X	X		X
1449	X	X		X		X	X	X		X
1900	X	X		X		X	X	X	X	X
2050			X	X		X	X	X	X	X
2351	X		X	X		X	X	X	X	X

MD\*: Measured depth, Abbreviations: Act: Actinolite, Ab: Albite, Anh: Anhydrite, Cal: Calcite, MLC: Mixed layer clay, Chl: Chlorite, Ep: Epidote, Py: Pyrite, Qz: Quartz, Wo: Wollastonite

In open spaces, the determination of paragenetic sequence is based on the principle of mineralization order. The mineral on the edges of fractures, veins or vesicles is older than the next layer. Then, as explained in Section 5.2.1, primary minerals are altered and replaced by secondary minerals. Therefore, in mineral replacement analysis, the replacing mineral is younger than the former primary mineral. Cross-cutting relationships in crystals also help with establishing the paragenetic sequence. Overprinting features and textural form in minerals also give information about the time and/or the temperature regime within the reservoir. Indeed, when a lower temperature mineral overprints a high temperature mineral, it indicates a change in the thermal regime towards cooling.

After analysis of alteration minerals under the petrographic microscope, their deposition sequences are detailed in Table 3. The observation shows that most of the hydrothermal minerals have been formed by replacement and reprecipitation. Vesicles and fractures were more difficult to determine, they probably crashed during the drilling due to the small size of the cuttings. The paragenetic sequences expose two different thermal regimes. A regime is prograde if higher-temperature minerals overprint or are formed after low-temperature minerals. In the case of Fiale 3, lower-temperature minerals (e.g. calcite, quartz, and anhydrite) are deposited after high-temperature ones such as actinolite, wollastonite or epidote. The deposition sequences suggest that the reservoir has experienced cooling.

TABLE 3: Sequence of mineral deposition in well Fiale 3

Depth m (MD)	Lithology	Mode of occurrence	Sequence from old to young
300	Basalt	Vesicle	Fine-grained clay - Calcite
450	Intermediate rock	Fracture/Replacement	Calcite
700	Intermediate rock	Vesicle Replacement	Chlorite - Anhydrite - Calcite Calcite - Quartz
851	Intermediate rock	Fracture Replacement	Calcite Albite - Epidote
1001	Intermediate rock	Vesicle Vein	Epidote - Chlorite Quartz
1151	Intermediate rock	Vesicles	Chlorite - Epidote Chlorite - Epidote - Calcite Fine-grained clay - Anhydrite - Calcite
1302	Intermediate rock	Vesicle Replacement	Calcite - Epidote - Quartz Epidote - Quartz Albite - Epidote Albite - Calcite
1449	Intermediate rock	Replacement	Albite - Epidote - Actinolite Albite - Calcite
1900	Basalt	Vein Replacement	Epidote Albite - Actinolite Epidote - Quartz
2050	Intermediate rock	Replacement Vesicle	Epidote - Wollastonite - Anhydrite Epidote - Chlorite - Quartz
2351	Acidic rock	Replacement	Albite - Actinolite - Anhydrite

### 5.3 Thermal history

To establish the thermal history of Fiale 3, a comparison of alteration minerals and measured temperatures has been undertaken to determine the current reservoir conditions in the geothermal well. In the present study, the hydrothermal alteration temperature curve was obtained from the first occurrence of the minerals and their formation temperature. The minerals used are smectite ( $\geq 40^\circ\text{C}$ ), quartz ( $\geq 180^\circ\text{C}$ ), chlorite ( $\geq 220^\circ\text{C}$ ), epidote ( $\geq 230^\circ\text{C}$ ), and actinolite ( $\geq 280^\circ\text{C}$ ). Measured temperatures and pressure were acquired from Turk et al. (2019) and Carver et al. (2019). The logs are presented in Figure 12.

The temperatures were measured approximately two months after completion of the well on 14<sup>th</sup> April 2019 and are compared to the alteration mineral temperatures. From the upper part to 390 m, the current temperature shows a slight cooling before reaching  $214^\circ\text{C}$  at 625 m (MD). This indicates a slight heating up compared to the quartz temperature ( $180^\circ\text{C}$ ). However, below this depth, high temperature minerals, e.g. epidote ( $\geq 230^\circ\text{C}$ ) and actinolite ( $\geq 280^\circ\text{C}$ ), occur at measured temperatures of  $150^\circ\text{C}$  and  $74^\circ\text{C}$ , respectively. This reflects a significant cooling of the reservoir between 733 m and 1700 m (MD). However, no mineralogical indications of the cooling are observed. In the lower part of the well, the current temperature increases progressively and follows approximately the boiling point curve (BPC) from 2500 m and 2625 m. A maximum temperature of  $362^\circ\text{C}$  was recorded at 2625 m (MD).

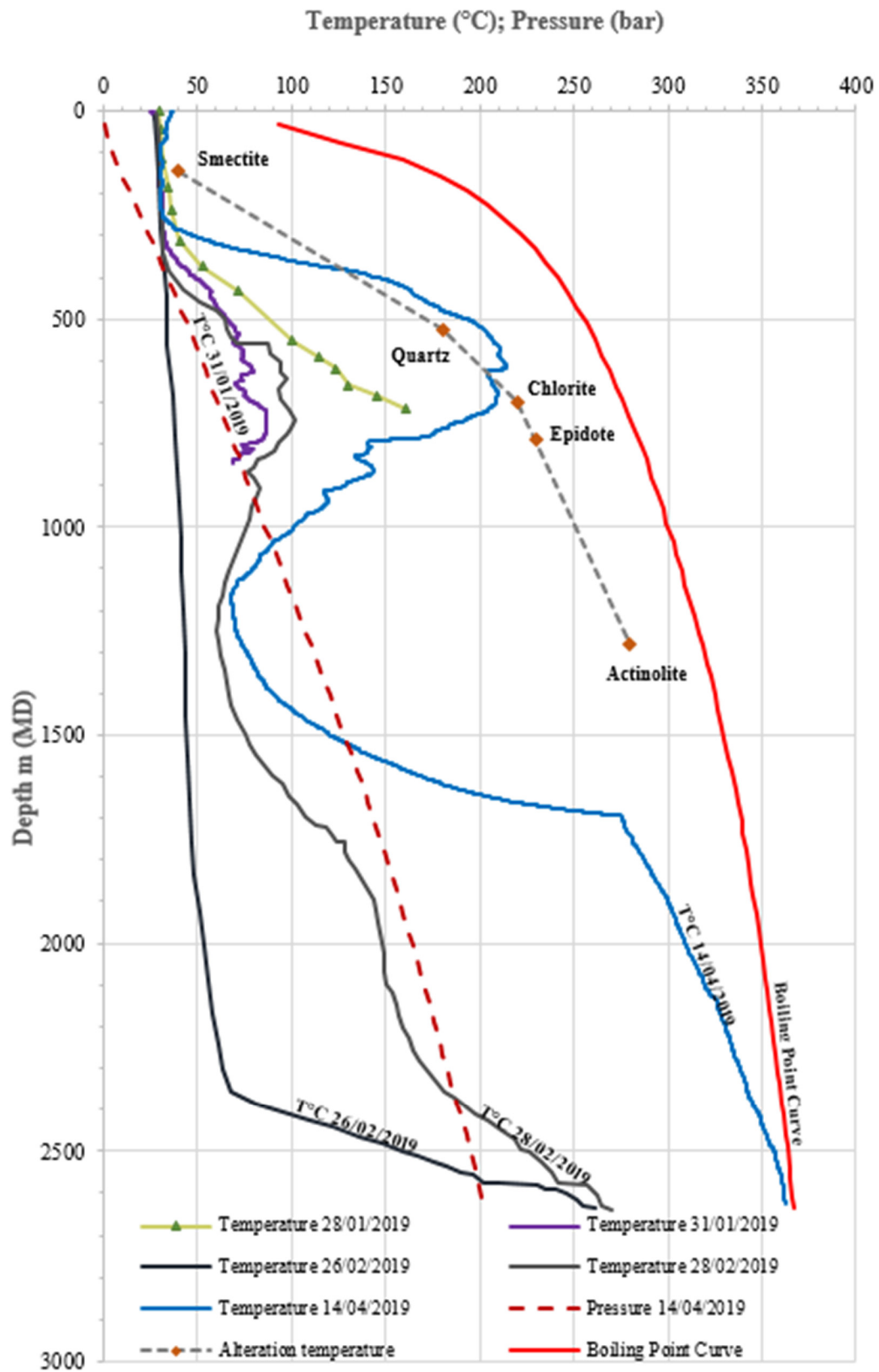


FIGURE 12: Temperature, alteration minerals, pressure and boiling point curve profiles of Fiale 3 (Turk et al., 2019; Carver et al., 2019)



### 5.4 Permeability zones

Feed zones are described as permeable layers able to produce significant amount of water. Aquifers refer to geological formations which can store and transmit water. The type of rock, permeability and the porosity are parameters that influence the flow of fluids. Two type of porosity exist. The primary one is formed during genesis of the rock such as voids and pores. The secondary porosity appears after the rock has formed such as the faults, joints, veins, or formation contacts (Reyes, 2000). Several parameters which are circulation losses and/or gains, temperature and pressure logs, rate of penetration, and alteration rate are used to identify permeable zones and aquifers/feed points in geothermal wells.

In well Fiale 3, the permeable zones are deduced mainly from circulation losses, temperature logs, alteration intensity based on the minerals indicative of permeability such as calcite or pyrite, and the results of the injection tests (Carver et al., 2019). The feed zones are described below and summarized in Table 4.

TABLE 4: Fiale 3 permeability zones

Depth m (MD)	Rock type	Size	Remarks
25-140	-	Small	Total loss of circulation
180-185	-	Small	Total loss of circulation
566-569	-	Small	Total loss of circulation
633	Basalt	Small	Fracture/vein, small cold inflow
733	Intermediate rock	Large	Faults with large intrusion of cold seawater, abundance of calcite and pyrite
817	Intermediate rock	Small	Fracture/vein, small cold inflow, abundance of calcite & pyrite
858	Intermediate rock	Small	Fracture/vein, small cold inflow, abundance of calcite & pyrite
933	Intermediate rock	Small	Fracture/vein, small cold inflow, abundance of calcite & pyrite
1700	Intermediate rock	Small	Fracture, small increase of temperature
1736-1749	-	Small	Total loss of circulation
2100	Intermediate rock	Small	Fluid losses, small inflow of hot water
2350	Acidic rock	Small	Fluid losses, small inflow of hot water
2580	Acidic rock	Small	Fluid losses, small inflow of hot water
2600	Acidic rock	Small	Small inflow of hot water
2650	Acidic rock	Small	Small inflow of hot water

During drilling, total losses of circulation have been experienced between 25 and 140 m, 180 and 185 m, 566 and 569 m, and 1736 and 1749 m depth. Temperature logs were obtained during and after drilling of the well. The results are presented by Carver et al. (2019). The temperature curves (Figure 12) show minor feed points at 633 m, 817 m, 858 m and 933 m. They are indicated by a small decrease in temperature caused by the intrusion of cold water. The largest inflow of cold seawater is at 733 m and results in a reversal of temperatures down to 1700 m. This depth interval has a high permeability controlled by the major NW-SE faults. Based on the alteration intensity observed during cutting analysis, this zone is associated to high amounts of calcite and pyrite in vein fillings. Two small feed zones are found at 2350 m and 2580 m. Spinner data (Carver et al., 2019) indicate fluid losses at the same depths and additionally at 2100 m.

Two injection tests have been carried out to test the permeability of the shallow reservoir between 500 and 850 m (Carver et al., 2019). The injectivity index (II) is 0.97 kg/s/bar. It indicates a low permeability. The last injection test was conducted on 26<sup>th</sup> and 27<sup>th</sup> February 2019 to estimate the permeability of the deep reservoir between 1730 and 2660 m that corresponds to the interval depth of the perforated liner. According to Carver et al. (2019), the injectivity index shows a low permeability with 0.50 kg/s/bar.

### 5.5 Correlation of Fiale wells and Asal 5

Stratigraphic correlation between wells Asal 5, Fiale 1, Fiale 2 and Fiale 3 was created using the Petrel software. The correlation results are mainly based on the stratigraphy of Asal 5 which is the most studied and described well in the Fiale caldera area (Aqater, 1989). Five stratigraphic units are found as shown in Figure 13. The upper part is formed by the recent volcanic unit of the Asal series. This unit consists dominantly of basalts. Then, the Afar stratoid series consist of basic and intermediate products. A thin sedimentary unit deposited during the Pliocene is found only in well Asal 5 and probably in Fiale 1. This layer marks the transition with the Dalha basalt unit. The Mabla rhyolite unit has been described in the Fiale wells based on cuttings analysis.

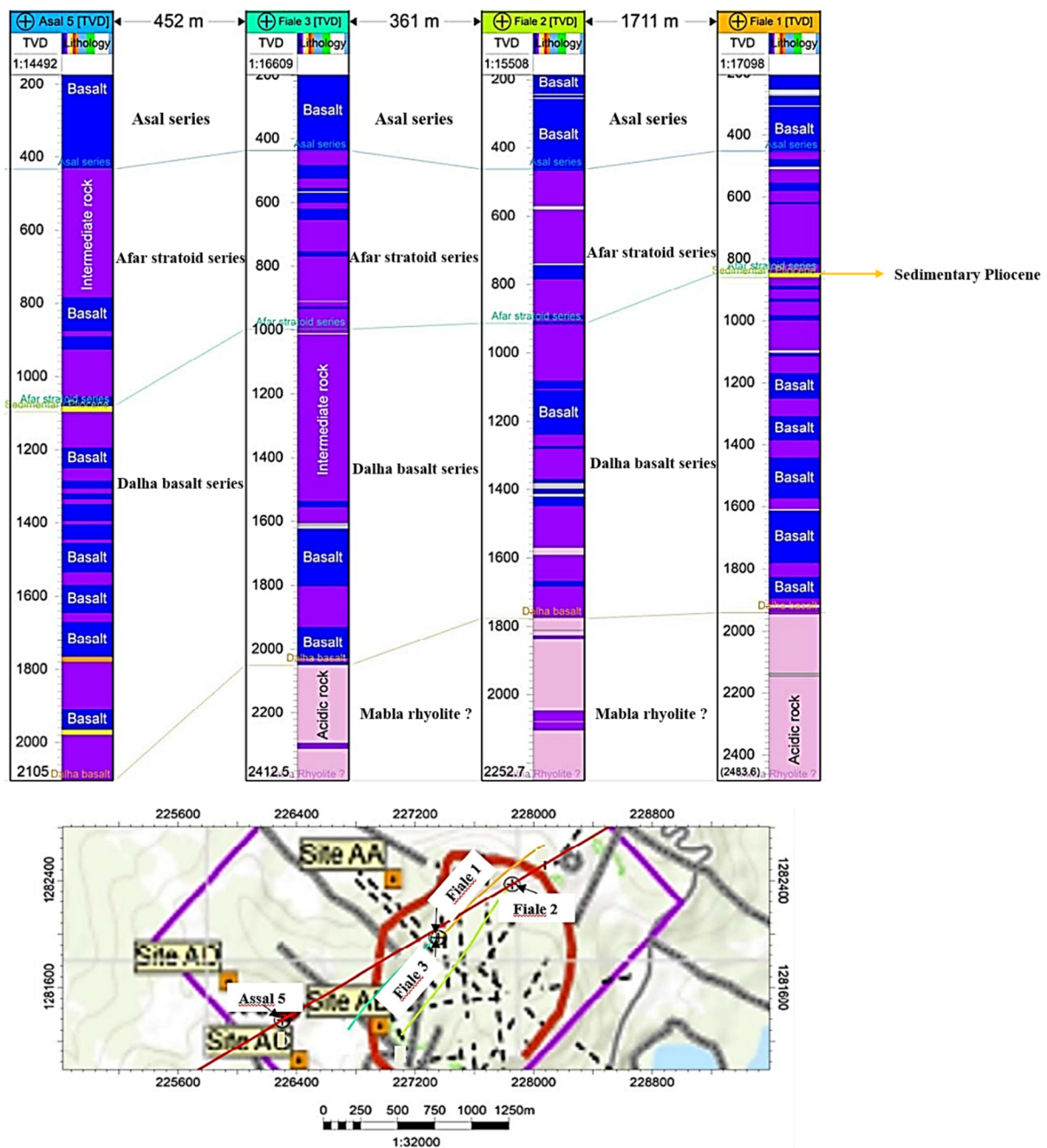


FIGURE 13: Stratigraphic correlation along a SW-NE cross-section between wells Asal 5, Fiale 1, Fiale 2 and Fiale 3. The lower image shows the location of the profile

Occurrence of hydrothermal alteration minerals in several wells can help to analyse changes in the reservoir. To observe the distribution of alteration minerals and consequently the evolution of the reservoir in the four wells of the Asal-Fiale geothermal field, a simple alteration model along a SW-NE cross-section was created with the Petrel software (Figure 14). Based on their equilibrium temperatures, smectite ( $\geq 40^\circ\text{C}$ ), quartz ( $\geq 180^\circ\text{C}$ ), chlorite ( $\geq 220^\circ\text{C}$ ), epidote ( $\geq 230^\circ\text{C}$ ), and actinolite ( $\geq 280^\circ\text{C}$ ) have been chosen to establish the alteration zones. Current isotherms of  $40^\circ\text{C}$ ,  $180^\circ\text{C}$ ,  $220^\circ\text{C}$ ,  $230^\circ\text{C}$ , and  $280^\circ\text{C}$  have been added to illustrate the actual thermal state of the geothermal reservoir. Fiale 1, Fiale

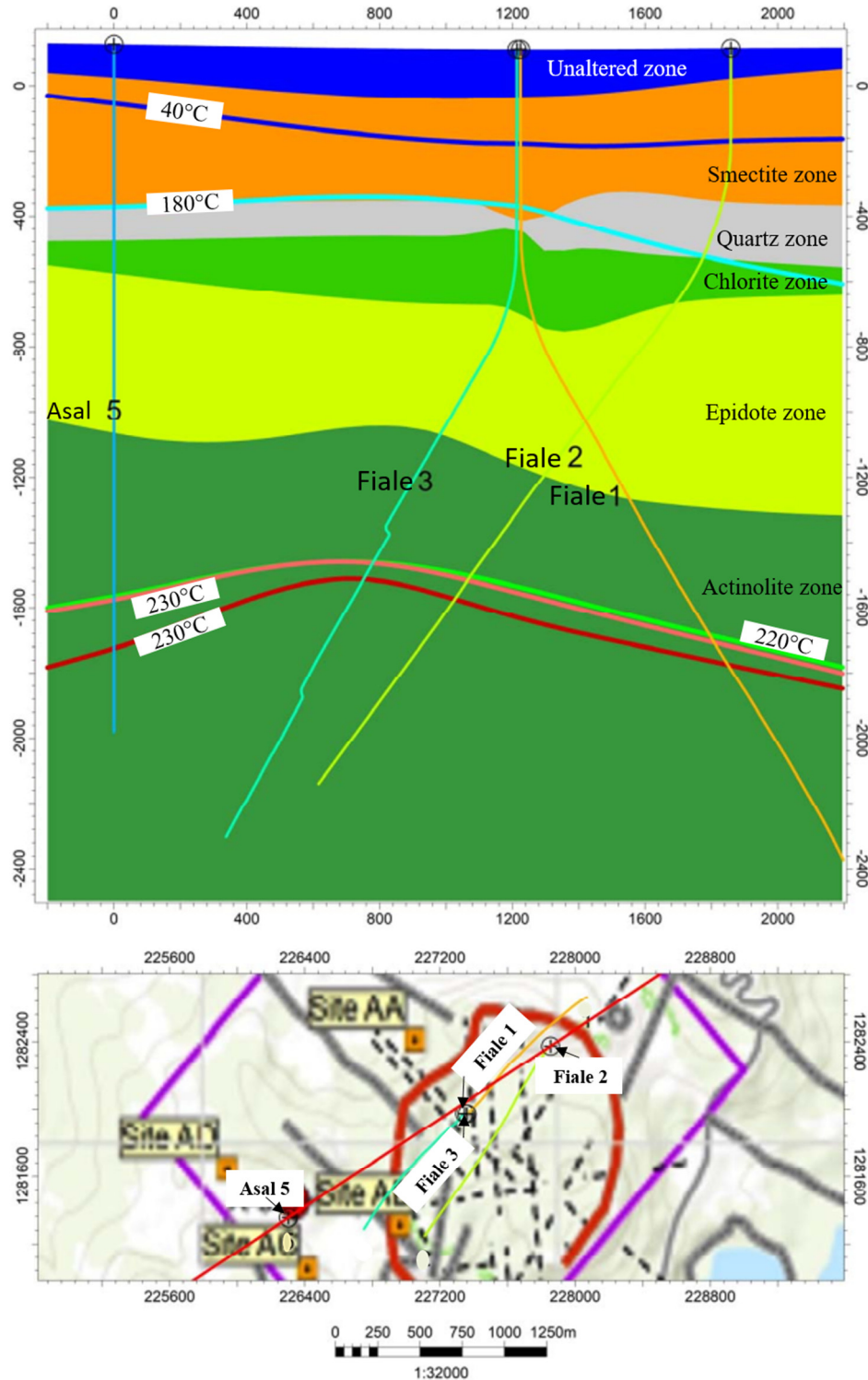


FIGURE 14: Alteration model (upper image) based on SW-NE cross-section between wells Asal 5, Fiale 1, Fiale 2 and Fiale 3. The lower image shows the location of the profile

2 and Fiale 3 are deviated wells and Asal 5 is the only vertical well located outside the caldera. The wells are approximatively at the same level.

The results as illustrated by the model in Figure 14 show that the quartz zone is uniform except for Fiale 1 and 3 which have a thicker smectite zone and slight up-doming of the chlorite zone below. The epidote zone appears at slightly higher depth in the south-western part around Asal 5 and at deeper depth around Fiale 2 before rising slightly in Fiale 1. The actinolite isograd is shallower in Asal 5 and Fiale 3 before rapidly lowering in Fiale 2 and Fiale 1. This indicates that the temperatures were higher near Fiale 3 but without a major upflow zone.

The isotherms obtained from measured temperatures in the wells, show a significant drop of the high temperatures. Indeed, 220°C, 230°C and 280°C isotherms are found at deeper depths below the actinolite isograd. This cooling is due to the large inflow of cold seawater into the system through the major rift faults but no evidence for a upflow zone is found. This could indicate that the Fiale caldera is in current state not an upflow zone, but rather shows characteristic patterns of an outflow zone.

## 6. DISCUSSION

Based on cutting analysis, the lithology of the well Fiale 3 consists mainly of fine- to medium-grained basaltic lava flows in the upper part of the well. Fine-to medium-grained intermediate rocks are found in the middle part intercalated with some basaltic rocks. The bottom is mainly formed by fine-to medium-grained acidic rocks. According to the stratigraphy correlation between the wells, four main stratigraphic units are found which are the Asal series, the Afar stratoid series, the Dalha basalt series and the Mabla rhyolite.

Petrographic observations permit to observe hydrothermal alteration minerals and to study their paragenetic sequences. Alteration minerals are mainly found as replacements of primary minerals and in assemblage. They also have been observed as filling in vesicles, veins, and rare fractures. They include calcite and pyrite which are used as indicators of permeability and are present in high amount between 450 and 1250 m (MD). High-temperature minerals increase with depth. Epidote appears at 792 m, actinolite at 1283 m and wollastonite at 1371 m. The distribution of hydrothermal alteration minerals indicates a prograde evolution of the temperatures in the well. However, anhydrite, which is a sulphate rich mineral, is identified from 700 m to deeper depth in the well. It shows that seawater has been heated up and led to the precipitation of the mineral.

By compiling binocular, thin sections, methylene blue and XRD analyses, five alteration zones were recognized. In order of increasing depth, they are the smectite zone (145-550 m), the chlorite zone (550-792 m), the epidote zone (792-1283 m) and the epidote-actinolite zone (1283-2660 m). The unaltered zone is in the upper part between the surface and 145 m (MD).

The occurrence of alteration minerals helped to establish the paleo-temperature curve. It is then compared to the measured temperatures and boiling point curves. It shows a significant temperature reversal between 733 and 1700 m caused by a large inflow of cold seawater (Figure 12). Moreover, this cooling is shown by the presence of anhydrite and rarely in sequences (Table 3). It is also important to note that the cold zone does not contain other low-temperature minerals. Below 1250 m, the temperature starts to increase progressively and follows the boiling point curve (BPC) in the lowest depths. A maximum temperature of 362°C was recorded at 2625 m (MD). The discrepancies between the alteration minerals and current temperatures indicate that Fiale 3 is not in state of equilibrium. Furthermore, the absence of lower temperature minerals in the cold zone could demonstrate that the inflow of cold seawater may be geologically young.



By analysing the measured temperature curves and reservoir testing results, feed zones are mainly associated to circulation losses in the shallow part of the well. The temperature profiles show also minor feed points at 633 m, 817 m, 858 m and 933 m indicated by minor cooling. The largest feed point is noted at 733 m (MD) causing the temperature reversal of Fiale 3. The cold inflow is explained by the infiltration of seawater from the Ghoubbet bay to the Asal Lake through the major NW-SE trending faults. Three more small feed points are found at 1741 m, 2100 m, 2350 m, and 2580 m. The injection tests show the existence of a shallow reservoir which is relatively hot between 500 and 850 m (MD). It has low permeability which is also found in the lower part of the well.

The simple alteration model has been created with the help of the Petrel software. The results show that the alteration zones are approximatively uniform throughout the Fiale caldera, except for a small up-doming of chlorite, epidote and actinolite isograds observed in well Fiale 3. This could indicate that the temperatures were higher in this zone but there is no evidence of a hot upflow zone. Comparing the current isotherms to the alteration isograds shows a significant cooling of the reservoir. The 220°C, 230°C and 280°C isotherms are observed below the actinolite isograd. The cooling of the reservoir is caused by the large inflow of cold seawater from Ghoubbet bay toward the Asal Lake through the NW-SE faults of the rift. A small up-doming of the isotherms is noticed near Fiale 3 at deep depths but again, no evidence of an up-flow zone is found. This could indicate that the Fiale wells and Asal 5 well are situated in an outflow zone.

## 7. CONCLUSIONS

The borehole study of well Fiale 3 has provided a first comprehensive overview of the lithology, alteration mineralogy, thermal history and permeability within the Fiale caldera. Based on the obtained results, the following can be concluded:

- The lithostratigraphy of Fiale 3 is divided into four stratigraphic units which are the Afar series in the upper part, the Afar stratoid series, Dalha basalt series and the Mabla rhyolite in the bottom of the well. The stratigraphic correlation is based on cuttings analysis and comparison with the Asal 5 well. Further analyses are needed to confirm the lithostratigraphy distribution in Fiale 3, the chemical nature of the stratigraphic units.
- Hydrothermal alteration minerals in well Fiale 3 are found as products of replacement of primary minerals and fillings in vesicles, veins and fractures. High temperature minerals such as albite, epidote, actinolite, and wollastonite are described. Anhydrite mineral is also observed from 700 m to deeper depths which is an indicator of seawater intrusion.
- In total, five alteration mineral zones are counted. They are the unaltered zone (0-145 m), the smectite zone (145-550 m), the chlorite zone (550-792 m), the epidote zone (792-1283 m) and the epidote-actinolite zone (1283-2660 m).
- The thermal history of Fiale 3 demonstrates a cooling of the geothermal system due to the large intrusion of cold seawater throughout the major NW-SE faults of the Asal-Ghoubbet rift. Anhydrite is an indicator of the cooling with regards to alteration mineralogy. However, low-temperature minerals are not observed by any applied method. The differences between alteration and measured temperatures may correspond to a recent cooling and high-temperature minerals are relicts of a former geothermal system with higher temperatures. Further analysis such as fluid inclusion analysis could help to better describe the impact of the reversal temperature within the geothermal system.
- The injection tests find evidence of two reservoirs. A shallow reservoir is located between 500 and 850 m with a maximum temperature of 214°C and low permeability. The second reservoir is located between 1783 and 2660 m and low in permeability. The largest feed zone corresponds to the inflow of seawater at 733 m. In general, it seems that the well has low permeability.
- Finally, the correlation of hydrothermal alteration zones and currents isotherms between Fiale wells and Asal 5 located outside the caldera show that the area is located in an outflow zone and

no indication for an active upflow zone exist. Moreover, the model also demonstrates the cooling of the geothermal system caused by the intrusion of cold seawater through the major faults of the Asal-Ghoubbet rift. Further geothermal exploration is needed to locate possible up-flow zones in the area.

### ACKNOWLEDGEMENTS

I would like to thank the United Nation University Geothermal Training Programme (UNU-GTP) and the Government of Iceland for granting me this great opportunity to participate in the six months training programme. Special thanks to the director of the UNU-GTP, Mr. Lúdvík S. Georgsson, deputy director, Mr. Ingimar G. Haraldsson, Ms. Thórhildur Ísberg, Ms. Málfríður Ómarsdóttir, Mr. Markús A. G. Wilde, and Dr. Vigdís Harðardóttir for their coordination and constant help during this course. I cannot forget to thank my employer, the Office Djiboutien pour le Developpement de l'Energie Geothermique (ODDEG), for giving me the chance to attend this rich training programme. I am grateful to my supervisor, Dr. Tobias Björn Weisenberger, for his guidance and mentoring during this research work. Special thanks go to Ms. Helga Margrét Helgadóttir, Ms. Sylvia Rakel Gudjónsdóttir, Ms. Anette K. Mortensen, Mr. Sigurdur Sveinn Jónsson for their presence and their support. I am grateful to the entire Iceland GeoSurvey (ÍSOR) staff who took part in the programme. Finally, I was happy to share this beautiful journey with the 2019 UNU fellows. Thank you for the good times, the laugh, the memories, and the hard work shared together. My sincere gratitude to my beloved family and friends back home in Djibouti for their support during these six months.

### REFERENCES

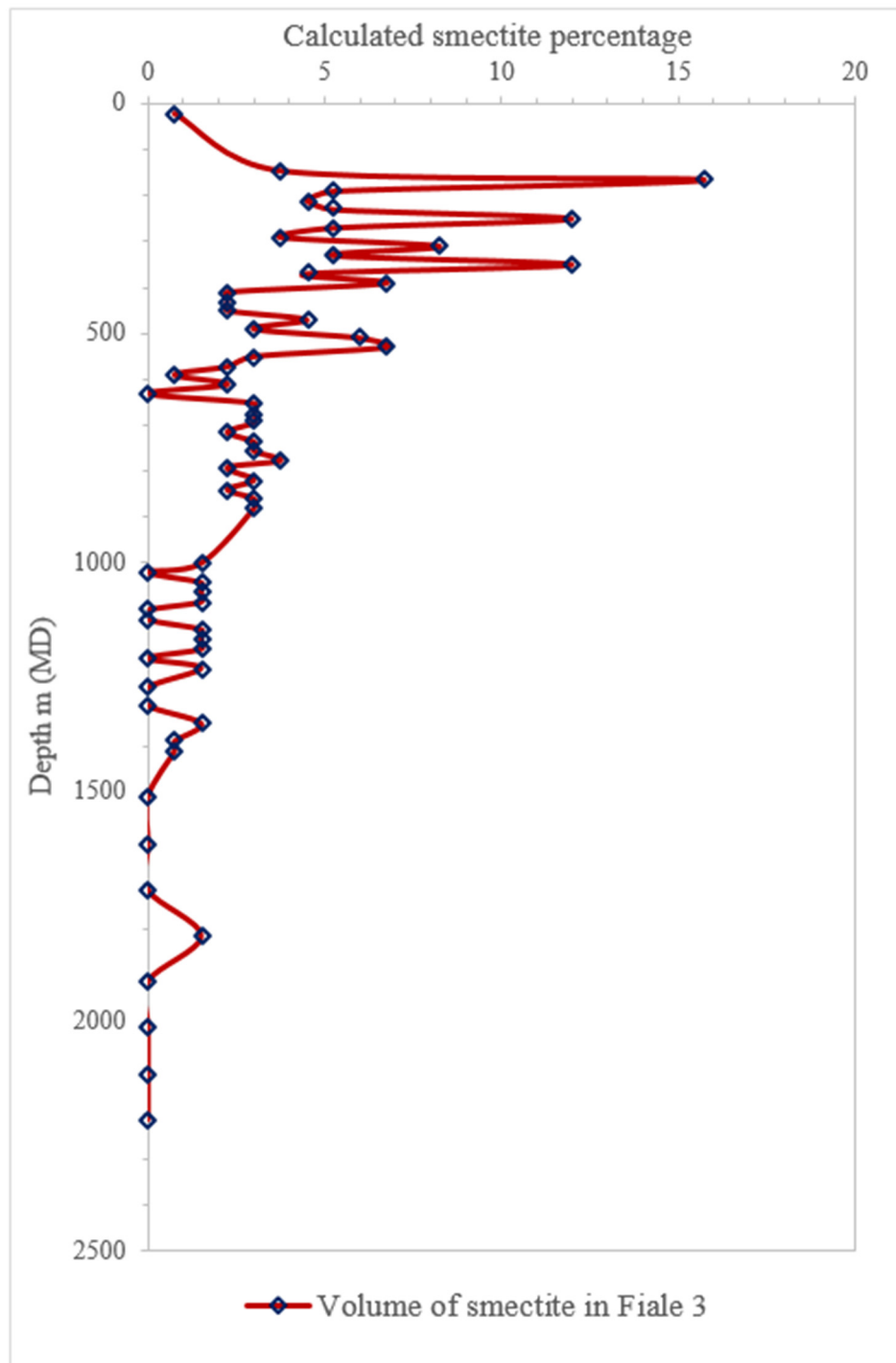
- Abdallah, A., Courtillot, V., Kasser, M., Le Dain, A.Y., Le'pine, J.-C., Robineau, B., Ruegg, J.-C., Tapponnier, P., and Tarantola, A., 1979: Relevance of Afar seismicity and volcanism to the mechanics of accreting plate boundaries, *Nature*, 282, 17–23.
- AfDB, 2013: *Geothermal exploration project in the Lake Assal region*. African Development Bank, Rabat, 31 pp.
- Ahmed, M., 2008: Borehole geology and hydrothermal mineralization of well HN-08, Hellisheidi geothermal field, SW-Iceland. Report 8 in: *Geothermal training in Iceland 2008*. UNU-GTP, Iceland 1-29.
- Aquater, 1989: *Djibouti geothermal exploration project, Republic of Djibouti*. Aquater S.p.a report A3770, 159 pp.
- Árnason, K., Björnsson, G., Flóvenz, Ó. G. and Haraldsson, E. H., 1988: *Geothermal resistivity survey in the Assal Rift in Djibouti. Volume I: Main text*. ÍSOR – Iceland GeoSurvey, report OS-88031/JHD-05, 49 pp.
- Árnason, K., Eysteinnsson, H. and Vilhjálmsson, A. M., 2008: *The Assal geothermal field, Djibouti. Geophysical surface exploration 2007–2008*. Iceland GeoSurvey, report ÍSOR-2008/019, 77 pp.
- Audin, L., Manighetti, I., Tapponnier, P., Me'tivier, F., Jacques, E., and Huchon, P., 2001: Fault propagation and climatic control of sedimentation on the Ghoubbet Rift Floor: Insights from the Tadjouraden cruise in the western Gulf of Aden, *Geophys. J. Int.*, 144, 391– 413.
- Barberi, F., Ferrara, G., Santacroce, R., Varet, J., 1975: Structural evolution of the Afar triple junction. In: Pilger, A., Rösler, A. (eds.), *Afar Depression of Ethiopia, vol. 1*. Schweizerbart, Stuttgart, Germany, 38–54.

- Bird, D.K., Schiffman, P., Elders, W.A., Williams, A.E., and McDowell, S.D., 1984: Calc-silicate mineralization in active geothermal systems. *Economic Geology*, 79, 671-695.
- BRGM, 1973: *Geophysical study using Melos surveys and electric surveys in the Lake Asal region (TFAI)*. BRGM office, Orléans, France, report (in French), 18 pp.
- Browne, P.R.L., 1978: Hydrothermal alteration in active geothermal systems. *Ann. Rev. Earth Planet. Sci.*, 6, 229-250.
- Carver, C.T., Garg, S.K., Davis, L.C., and Jalludin, M., 2019: Reservoir characterization from exploration well completion tests in the Fiale caldera, Djibouti. *Geothermal Resources Council, Transactions*, 43, 14 pp.
- Courtillot, V., Armijo, R., and Tapponnier, P., 1987: Kinematics of the Sinaiuml; Triple Junction and a two-phase model of Arabia-Africa rifting. In: Coward, M.P., Dewey, J.F., and Hancock, P.L. (eds.), *Continental Extensional Tectonics, Geol. Soc. Spec. Publ.*, 28, 559–573.
- Courtillot, V., Jaupart, C., Manighetti, I., Tapponnier, P. and Besse, J., 1999: On causal links between flood basalts and continental breakup. *Earth Planet. Sci. Lett.*, 166, 177–195.
- De Chabaliér, J.-B., and Avouac, J.-P., 1994: Kinematics of the Asal Rift (Djibouti) determined from the deformation of Fiale Volcano, *Science*, 265, 1677– 1681.
- Demange, J. and Puvilland, P., 1990 : *Champ géothermique d'Assal, Djibouti; synthèse des données*. BRGM, report (in French).
- Demange, J., Stieltjes, L., and Varet, J., 1980: L'éruption d'Asal de Novembre 1978. *Bull. Soc. Geol. Fr.*, 7, 837– 843.
- Dobre, C., Manighetti, I., Dorbath, C., Dorbath, L., Jacques, E., & Delmond, J., 2007: Crustal structure and magmato-tectonic processes in an active rift (Asal-Ghoubbet, Afar, East Africa): 1. Insights from a 5-month seismological experiment. *J. Geophysical Research*, 112.
- Henley, R. W., and Ellis, A.J., 1983: Geothermal systems ancient and modern: a geochemical review. *Earth Science and Reviews*, 19, 1-50.
- ISERST, 1985: Carte géologique de la République de Djibouti à 1:100,000: Tadjoura (in French). République de Djibouti.
- ISERST, 1986: Carte géologique de la République de Djibouti à 1:100,000 : Ali Sabih (in French). République de Djibouti.
- Khodayar, M., 2008: *Results of the 2007 surface geothermal exploration in the Assal Rift and transform zones, Djibouti. Tectonics and Geothermal manifestations*. ÍSOR - Iceland GeoSurvey, report ÍSOR-2008/008, 70 pp + annex + 5 maps.
- Kristmannsdóttir, H., 1976: Type of clay minerals in hydrothermally altered basaltic rocks. *Jökull*. 26, 30-39.
- Kristmannsdóttir, H., and Tómasson, J., 1978: Zeolite zones in geothermal areas in Iceland. In: Sand, L.B., and Mumpton (eds.), *Natural zeolites, occurrence, properties, use*. Pergamon Press Ltd., 277-284.
- Le Gall, B., Daoud, A.M., Maury, R., Gasse, F., Rolet, J., Jalludin, M., and Moussa, N., 2015: *Geological map of the Republic of Djibouti*. CERD, Djibouti.
- Manighetti, I., Tapponnier, P., Gillot, P.-Y., Jacques, E., Courtillot, V., Armijo, R., Ruegg, J.-C., and King, G., 1998: Propagation of rifting along the Arabia-Somalia plate boundary into Afar. *J. Geophys. Res.*, 103, 4947–4974.
- Manighetti, I., King, G.C.P., Gaudemer, Y., Scholtz, C.H., and Dobre, C., 2001a: Slip accumulation and lateral propagation of active normal faults in Afar, *J. Geophys. Res.*, 106, 13,667– 13,696.

- Manighetti, I., Tapponnier, P., Courtillot, V., Gallet, Y., Jacques, E. and Gillot, Y., 2001b: Strain transfer between disconnected, propagating rifts in Afar, *J. Geophys. Res.*, 106, 13,613– 13,665.
- Marks, N., Schiffman, P., Zierenberg, R.A., Franzson, H., and Fridleifsson, G.Ó., 2010: Hydrothermal alteration in the Reykjanes geothermal system: Insights from Iceland deep drilling program well RN-17. *J. Volcanol. & Geothermal Research*, 189, 172-190.
- Moore, D.M., and Reynolds Jr., R.C., 1989: *X-ray diffraction and identification and analysis of clay minerals* (18<sup>th</sup> ed.). Oxford University Press, Oxford, 378 pp.
- Ngoc, P.V., Boyer, D., Mouel, J.L. and Courtillot, V., 1981: Identification of a magma chamber in the Ghoubbet-Asal Rift (Djibouti) from a magnetotelluric experiment. *Earth and Planetary Science Letters* 52, 372–382.
- Pinzuti, P., 2006: Croissance et propagation des failles normales du rift d'Asal-Ghoubbet par datations cosmogéniques <sup>36</sup>Cl-Liens avec le magmatisme (in French). Institut de Physique du Globe de Paris, PhD thesis.
- Reyes, A.G., 2000: *Petrology and mineral alteration in hydrothermal systems: from diagenesis to volcanic catastrophes*. UNU-GTP, Iceland, report 18-1998, 77 pp.
- Ruegg, J.-C., Le'pine, J.-C., and Tarantola, A., 1979: Geodetic measurements of rifting associated with a seismo-volcanic crisis in Afar. *Geophys. Res. Lett.*, 6, 817–820.
- Spürgin S., Weisenberger T.B., and Marković M., 2019: Zeolite-1 group minerals in phonolite-hosted deposits of the Kaiserstuhl volcanic complex, Germany. *Am. Min.*, 104, 659-670.
- Stefánsson, A., Gíslason, S.R. and Arnórsson, S., 2001: Dissolution of primary minerals in natural waters. II. Mineral saturation state. *Chemical Geology*, 172, 251-276.
- Stein, R., Briole, P., Ruegg, J.-C., Tapponnier, P., and Gasse, F., 1991: Contemporary, Holocene, and Quaternary deformation of the Asal Rift, Djibouti: Implications for the mechanics of slow spreading ridges, *J. Geophys. Res.*, 96, 21, 789–21,806.
- Tapponnier, P., Armijo, R., Manighetti, I., and Courtillot, V., 1990: Bookshelf faulting and horizontal block rotations between overlapping rift zones in southern Afar. *Geophys. Res. Lett.*, 17, 1–4.
- Tarantola, A., Ruegg, J.-C., and Lépine, J.-C., 1979: Geodetic evidence for rifting in Afar: A brittle-elastic model of the behaviour of the lithosphere, *Earth Planet. Sci. Lett.*, 45, 435– 444.
- Tarantola, A., Ruegg, J.-C., and Lépine, J.-P., 1980: Geodetic evidence for rifting in Afar, 2. Vertical displacements, *Earth Planet. Sci. Lett.*, 48, 363–370.
- Thorbjörnsson, D., Hersir, G.P., Gałeczka, I.M., and Richter, B., 2017: *Assal geothermal area, Djibouti, Conceptual Model*. ÍSOR - Iceland GeoSurvey, report ÍSOR-2017/089, 17-0091, 76 pp.
- Turk, J., Haizlip, J., Mohamed, J., Mann, M., Letvin, A., and Moussa, N., 2019: A comparison of alteration mineralogy and measured temperatures from three exploration wells in the Fiale caldera, Djibouti. *Geothermal Resources Council, Transactions*, 43, 11 pp.
- Varet, J., 1978: *Geology of central and southern Afar (Ethiopia and Djibouti Republic)*. Centre Natl. de la Res. Sci., Paris, 124 pp.
- Verhoef, P.N.W., 1992: The methylene blue adsorption test applied to geomaterials. *Memoirs of the Centre of Engineering Geology in the Netherlands, Delft University of Technology, No. 101, GEOMAT.02*, 70 pp.
- Weisenberger T., and Selbekk R.S., 2009: Multi-stage zeolite facies mineralization in the Hvalfjörður area, Iceland. *Int. J. Earth Sci.*, 98, 985-999.



**APPENDIX I: Relative volume of smectite clays in 2 g of rock as a function of depth, graph derived using the methylene blue test**



APPENDIX II: Results of XRD analyses

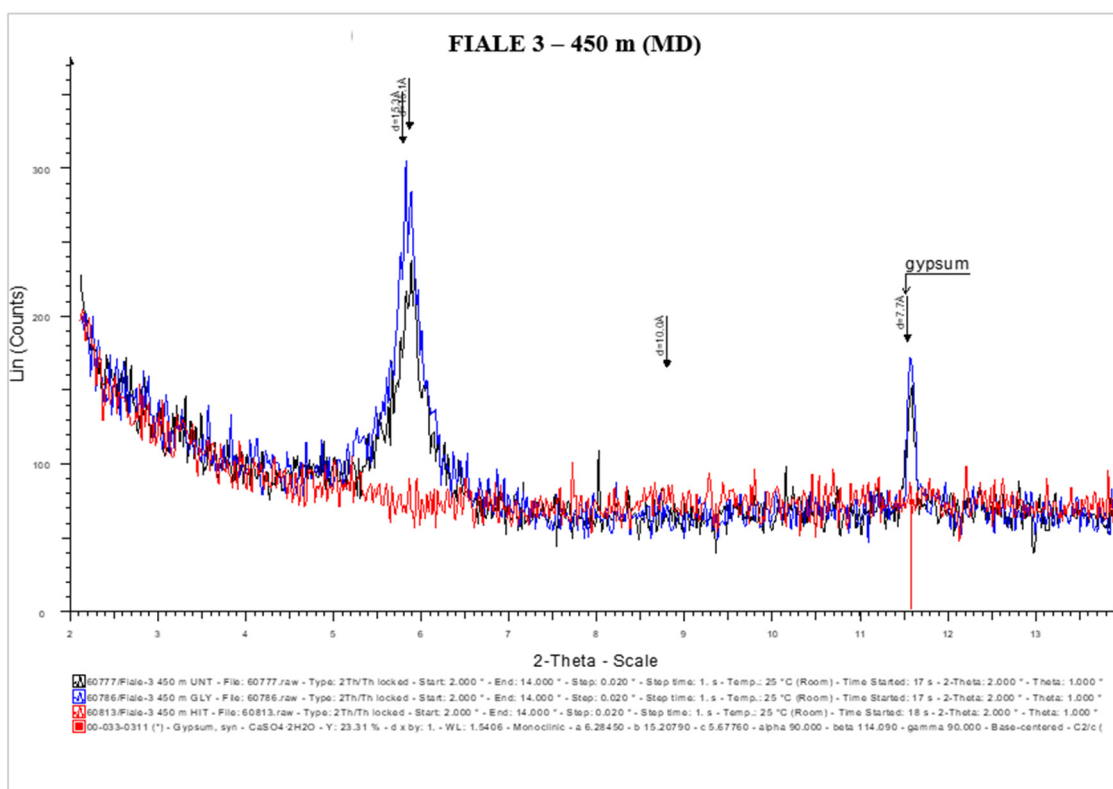


FIGURE 1: Occurrence of smectite (15.1 – 10 Å) and gypsum/anhydrite (7.7 Å)

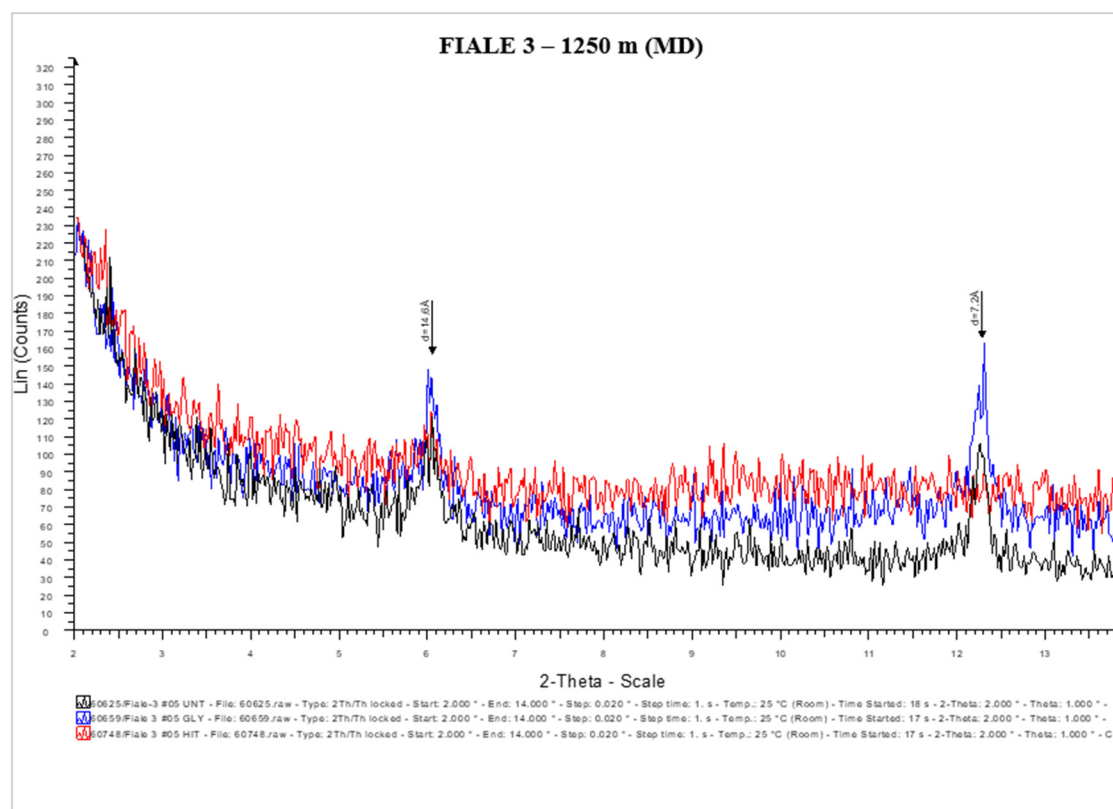


FIGURE 2: Occurrence of chlorite (14.6 – 7.2 Å)